The Correlation between the Penetration Force of Cutting Fluid and Machining Stability

by

Zhe Wang

A Thesis

Submitted to the Faculty

of the

Worcester Polytechnic Institute

In partial fulfillment of the requirements for the

Degree of Master of Science

in

Manufacturing Engineering

May 2010

Approved:

____

Professor Mustapha S. Fofana, Advisor

____

Professor Richard D. Sisson, Director of Manufacturing and Material Engineering

Abstract

The purpose of this thesis is to investigate the correlation between the penetration force of cutting fluids and machining stability. General studies are made to understand the classification of cutting fluids based on their chemical compositions. It is summarized why the proper selection of cutting fluid for different machining processes is important. The role of cutting fluids in machining process is documented as well as other related issues such as delivery methods, storage, recycling, disposal and failure modes. The uniqueness of this thesis is that it constructs a new mathematical model that would help to explain and quantify the influence of the penetration force of cutting fluid on machining stability. The basic principles of milling process, especially for thin wall machining are reviewed for building the mathematical model. The governing equations of the mathematical model are derived and solved analytically. The derived solutions are used to construct the stability charts. The results show that there is a direct correlation between the machining stability and the changes of the penetration force of the cutting fluid. It is shown that the machining stability region is narrowed as the penetration force of the cutting fluid increases while other machining variables are assumed to be constant. This narrowness of the stability region is more obvious at spindle speed over 6000 rpm.

Acknowledgements

Firstly, I would like to thank my advisor and my friend Professor Fofana. He has devoted a lot to guide me through this thesis and my past two years of study here at Worcester Polytechnic Institute. Then I would like to thank my parents who always support me with love through my life. And I would like to thank Hui Cheng for her love and support and tolerance during the preparation of this thesis. Finally my sincere appreciation is extended to committee members of the thesis - Professor Sisson and Professor Rong for their valuable support and contribution.

Table of Contents

List of Figures

List of Tables

Chapter 1. Machining and Cutting Fluids

Cutting fluid, as a component of machining industry, has been introduced and applied for over 100 years. It is believed that W. H. Northcott is probably the first man to mention the improvement in productivity that can be achieved when cutting fluid is applied in machining process. This observation is published in his book “A Treatise on Lathes and Turning” in 1868 (see 2). In 1907, F. W. Taylor pointed out that by applying a heavy water stream on the tool/workpiece interface, the cutting speed can be increased significantly by 30%-40% (see 45).

Since then, the technology of cutting fluids has been developed rapidly. Mineral, vegetable and animal oil have all been introduced, which played important role in enhancing various aspects of machining properties, including corrosion protection, antibacterial protection, lubricity, chemical stability and even emulsibility. However, due to the increasing cost of petroleum products, manufacturers starts to look for some substitutes for oil, which accelerates the development of water-based fluids with different chemical compositions performing different machining tasks. This effort also stimulates the use of synthetic or semi-synthetic water-based fluids that contain only little or even no oil. Study shows that water-based cutting fluids are now used in 80%-90% of all machining applications [1].

Cutting fluids play an important role in modern machining industry. They can impact the improvement of the surface finish, tool life and productivity significantly. Due to the importance of cutting fluids, significant issues have been raised in their application, recycling and disposal. Proper selection and application can reduce manufacturing cost and improve productivity. On the other hand, manufacturing failure and wastes can be experienced by misuse of cutting fluids. And regarding to the environmental impacts and health hazards by cutting fluids, recycling and disposal of cutting fluid are also of great importance. Improper disposal actions can cause severe health and environmental problems. Such actions can even lead the substantial penalty level against companies by the government agencies [2].

Numerous studies have been conducted to either investigate the impacts of the cutting fluid on machining process or set up evaluation criteria to assist proper selection and application of the cutting fluid. The goal of this thesis is to review and evaluate cutting fluid related issues such as classification, functions, penetration forces and their impact on machining processes. And due to the complexity of cutting fluid and many issues that come with the application of cutting fluid, the thesis focus on investigating the correlation between the penetration force of cutting fluid and the machining stability. The mathematical model representing milling operation is constructed. The governing equations of the motion are solved analytically to establish a direct correlation between the penetration force of cutting fluid and the regimes of milling stability. As a result, machining stability charts are constructed and in each of the charts stable spindle speed are identified in terms of the correlation between the penetration force of cutting fluid and milling stability.

The thesis is organized into seven chapters. Chapter 1 introduces the history and modern development of cutting fluids and the purpose and structure of the thesis. Chapter 2 studies the classification of cutting fluids and their impact on the machining processes. Chapter 3 presents the role of cutting fluids in machining processes and other related issues based on the literature and our own experience in working at WPI machine shop. Chapter 4 contains the performance evaluation of cutting fluids by previous researchers and reviews the classical milling processes. Chapter 5 describes the unique mathematical model, its governing equations, and presents the stability charts. Chapter 6 contains the results and discussions. In Chapter 7 we summarize the correlation between the penetration force of cutting fluid and machining stability.

Chapter 2. Classification of Cutting Fluids

2.1. General Classification

At the very first part of studying cutting fluid, it is of great importance to know what kinds of cutting fluid are currently available in the market. This will provide an opportunity to understand the forms and composition of the cutting fluid. Cutting fluids have been an integral part of machining industry for many years. Numerous kinds of cutting fluids are available in today's market. They range from oil-based cutting fluid to water-based [3]. Figure 1 summarizes the classification of cutting fluids. All of these types of fluids are widely used in a variety of machining operations. Among these fluids, synthetic fluids and semi-synthetic fluids are most suitable at high speed machining.

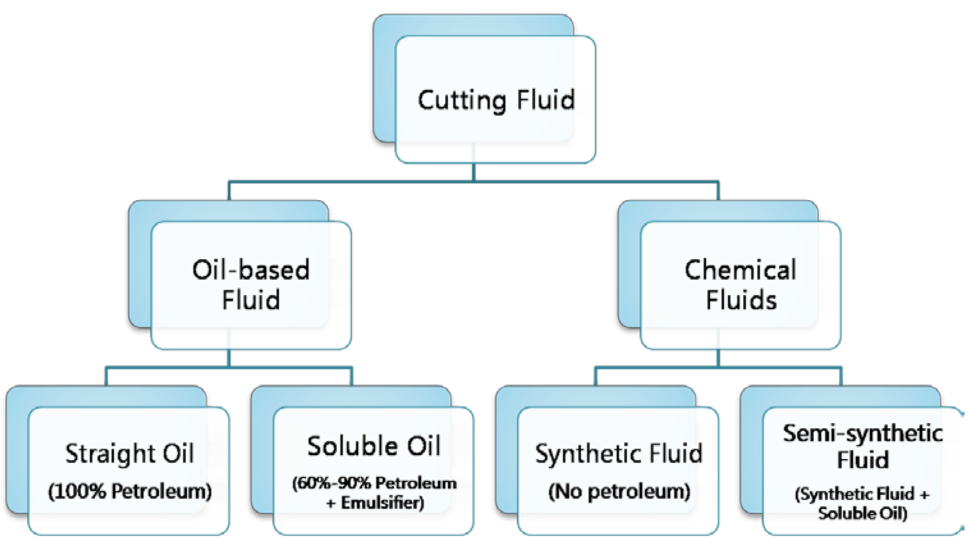

Figure 1: Classification of cutting fluids

2.2. Classification of Oil-based Fluids

Oil-based fluids can be sub-categorized into two types: straight oils and soluble oils. Straight oils which contain no water are 100% petroleum or mineral oils. Some may have particular additives to enhance their properties. Additives such as sulfur, chlorine or phosphorus can improve the wettability, lubrication and antiwelding properties of oils. The advantages of the straight oils include excellent lubrication, good rust protection, good sump life, easy maintenance and rancid resistant. The disadvantages include poor heat dissipation, increased risk of fire and oily film on workpiece. The application of this type of oil-based fluids is limited to low-speed and severe cutting operations.

Soluble oils which are also called emulsifiable oils or water-soluble oils are 60%-90% petroleum or mineral oils mixed with emulsifiers and other additives. The oils are mixed with water and the emulsifiers cause the oil to distribute in the water thereby forming an “oil-in-water” emulsion [4]. The advantages of the soluble oils include good lubrication, improved cooling capabilities and good rust protection. This type of soluble oils can be used for light to heavy duty operations. The disadvantages are more susceptible to rust problems, bacterial growth, tramp oil contamination and evaporation losses. They may form precipitates on machine, misting and oily film on workpiece. And all of this would impact maintenance cost.

2.3. Classification of Chemical Fluids

Chemical fluids can be sub-categorized into two types: synthetic fluids and semisynthetic fluids. Synthetic fluids contain no petroleum or mineral oils. It is provided as a concentrate and mixed with water before use. Synthetic fluids can be further classified as simple, complex or emulsifiable synthetic fluids based on their components [5]. The advantages of the synthetic fluids are excellent microbial control, resistance to rancidity, nonflammable and good corrosion control. The superior cooling qualities of the synthetic fluids and their easy separation from the workpiece and chips prolong tool life and improve the quality of machining applications. The disadvantages are reduced lubrication and may cause misting, emulsify tramp oil and form residues. This contaminants have adverse effects on machining operations.

Semisynthetic fluids which are also called semi-chemical fluids are a hybrid of soluble oils and synthetic fluids. Basically they contain small portion of mineral oils ranging from 2%-30% [6]. The balance portion mainly contains emulsifier, additives, agents and water. The advantages of semisynthetic fluids include good microbial control, resistance to rancidity and nonflammable. They have good corrosion control, good cooling and lubrication. This form of fluid can be easily separated from workpiece and chips. The disadvantages are water hardness impacts stability and may cause misting, foaming and allergy, emulsify tramp oil and form residues.

2.4. Cutting Fluid Impacts on Machining Processes

The proper selection the cutting fluid is very critical for enhancing machining processes performances. Different types of cutting fluids can deliver various kinds of impact on the machining processes. There are substantial evidences in the literature why the inappropriate use of cutting fluid will reduce the quality of machining operations.

J.M. Vieira et al. [36] have concluded in their paper that for high speed machining of AISI 1020 steel under the cutting condition: 100-220 m/min for cutting speed, 0.1-0.25

mm/tooth for feed rate and 1.0-2.5 mm for depth of cut, semi-synthetic fluids will deliver the best cooling results. Their study also indicated that the best surface roughness was achieved when dry machining. This gives us the potential assumption that the cutting fluid could possibly affect the machining stability so as to degrade the machining quality. Xavior et al. [37] also conducted an experiment among coconut oil, soluble oil and straight oil for testing their impacts on the surface roughness and tool wear on AISI 304 stainless steel under the cutting condition: 38.95/61.35/97.38 m/min for cutting speed, 0.5/1.0/1.2 mm for depth of cut and 0.2/0.25/0.28 mm/rev for feed rate. Their results indicated that coconut oil performs better than the other two in terms of tool wear and surface roughness. Belluco et al. [38] performed a drilling test on austenitic stainless steel under the cutting condition: 25 m/min for cutting speed, 0.1 mm/rev for feed rate and 33 mm for the total drilling depth using vegetable-based oil and mineral oil. They observed that vegetable-based oil produced better results than the mineral reference oil, the best performance being 177% tool life increase and 7% reduction in thrust force with respect to the commercial mineral oil. The results reflected not only the machining performance improvement but also potential advantages for environmental concerns.

As a result, it can be seen that for different machining operations and cutting conditions, the proper selection of cutting fluid is of great importance to maintain the machining stability and quality.

In the next chapter, the roles of cutting fluids will be documented. They include the basic functions of cutting fluid, delivery methods, storage, recycling, disposal and possible failure modes. Real machining cases are also examined briefly in terms of these issues mentioned above.

Chapter 3. Roles of Cutting Fluids in Machining Processes

3.1. General Concepts

In the previous chapter, we generally reviewed the classification of cutting fluids and evaluated on their impact on the machining processes. To understand cutting fluids, tt is of great importance to study their roles in machining processes as well.

Typically, cutting fluids play various roles during machining processes. The roles include four main aspects which are cooling, lubrication, corrosion protection and chip removal. To understand the roles of cutting fluids in process machining, we review the deformation and friction in the cutting process. For simplicity, cutting forces involved in a cutting operation are always examined in terms of an orthogonal cutting geometry shown in Figure 2.

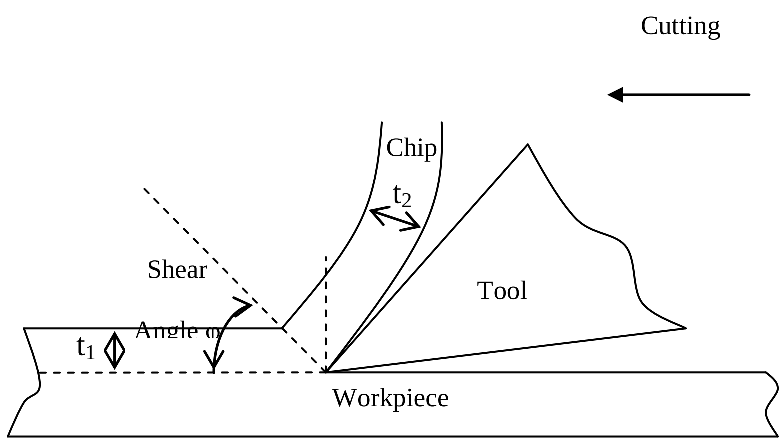

Figure 2: Orthogonal cutting geometry

One parameter that is usually mentioned when talking about machining process is the cutting ratio. It is the ratio of depth of cut to thickness of chip. If the depth of cut is kept constant, as the shear angle increases, one can easily see that the thickness of the chip will decrease accordingly. This in turn reduces the cutting force. Consequently, the power required per unit volume of metal and the heat generated will be reduced as well.

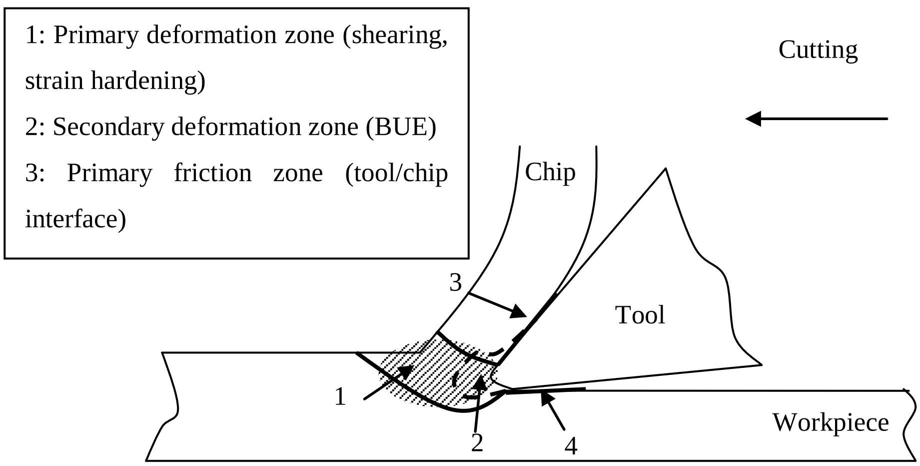

Figure 3: Orthogonal cutting deformation and friction zones

Figure 3 shows that there are four principle deformation zones along the tool/workpiece and tool/chip interfaces. The primary deformation zone is where the most energy is consumed during deforming. If the shear angle increases, the volume of primary deformation zone will likely be reduced.

The secondary deformation zone is where the built-up edge (BUE) forms. The BUE is a wedge-shaped quantity of workpiece material melted to the tip of the tool. It is usually even harder than the workpiece itself as a consequence of the strain hardening characteristics of the workpiece material. If the BUE is relatively large, it can decrease the effective rake angle and constantly degrade the finish quality of the workpiece surface by forming and breaking away. By selecting a proper cutting fluid, the BUE can be controlled to some extent.

Sliding friction would be another source of power consumption in cutting process. It occurs at both the tool/chip interface and the tool/workpiece interface. Tool/chip friction can be more significant than tool/workpiece friction, which can be a cause of rake wear of the tool. Tool/workpiece friction appears to be a cause of flank wear of the tool.

3.2. Basic Functions of Cutting Fluids

The basic functions of cutting fluids typically include the following four considerations: cooling, lubrication, corrosion protection and chip removal which are going to be discussed in detail below.

a) Cooling

It is known that the energy generated in metal cutting operation both through deformation and sliding friction process appears to be thermal energy or heat. It is also indicated that over 60% of the thermal energy is generated in primary deformation zone; while the rest is generated in secondary deformation zone and sliding friction zones [7]. The only advantage of the heat generated in cutting process is that it could reduce a limited amount of forces required for deformation of the workpiece. However this advantage is too limited compared with its disadvantages. The high temperature can usually shorten the tool life, cause an undesirable surface finish and bring down the cycle time due to the reduction of cutting speed. Basically, a cutting fluid should at least acquire two key abilities to dissipate heat in good time during cutting process. One is to gain access to the sources of heat and the other is to have the thermal capability to bring heat away.

It is still not quite clear about how a cutting fluid make penetration into the deformation and sliding friction zones. Several mechanisms have been proposed to model the penetration process. It is believed that more than one such mechanism take actions at the same time. However it appears that cutting fluids do penetrate and thereby causing heat dissipation.

And to remove the heat, the cutting fluid should have the following capabilities: thermal conductivity, specific heat, heat of vaporization and wettability with metal surfaces. Water-based fluids and dilute emulsions have a significant advantage over oil-based fluids in terms of thermal properties since water has a higher thermal conductivity than organic oil. It is widely recognized in high-speed machining that water-based fluids are used effectively. Vaporization is an effective way to remove heat since a large amount of thermal energy generated by deformation and friction will transform fluid from liquid state to gas state. It is also of great importance that the cutting fluid is capable to wet the surface of the workpiece, since it will determine the effective cooling area. For this capability, it is good for the fluid to have a low surface tension so that it can spread on more area rather than only forming beads.

To validate the heat dissipation mechanism, monitoring the tool life change could be an effective way as we mentioned previously. Other experiments indicate that increasing fluid penetration and applying high-pressure jets can enhance the cooling capabilities as well.

b) Lubrication

It is believed that due to high pressure and relatively high temperature in most cutting operations, liquid film cannot be sustained along tool/workpiece interface for all the time. Thus the conditions in a typical cutting process are believed to approach boundary lubrication. In boundary lubrication, additives in the cutting fluid react with both the workpiece material and the tool material to form chemical products on the interface. This process is thought to include two interrelated mechanisms. First, the lubricant absorbs into the chip surface and restricts the adhesion of chip material to the tool. Second, reactive components of the fluid combine chemically with the freshly generated metal surface of the chip to produce a film of lower shear strength than that of the chip material, thus reducing sliding friction, forces and temperature. Extreme pressure additives are often used to fulfill this function. Effective boundary lubrication must achieve the requirements, namely the quantity of fluid additive should be sufficient to take effects; the reactive composites in the additive should be available at the interface; the temperature should be high enough to catalyze the reaction but not too high to make the compound decompose or melt; the sliding speed should be relatively slow to allow enough time for reaction to occur. Therefore if high cutting speed is applied, the fluid accessibility would be limited, time for surface reaction will be decreased and some lower-melting-point compound cannot be used. Most commercial cutting fluids employ compounds of chlorine or sulfur as extreme pressure additives.

c) Corrosion Protection

It is of great importance to protect the workpiece from corrosion damage. One method used to control the corrosion is to add soda ash to the cutting fluid, which will likely increase the alkalinity of the fluid and reduce the possibility of rust.

Mineral oils are found to be a great deterrent to rust, which is able to form a physical film along tool/workpiece interface to prevent chemical reaction from occurring. However, along with the increase of cutting speed and hardness of the material, the straight mineral oil may lack the ability to wet the machining surface. Thus some polar compound additives are added to form emulsifiable oils. These emulsifiable oils combine the cooling properties of water and lubrication abilities of mineral oil. These fluids as well as semi-synthetic fluids are alkaline in nature to prevent workpiece surface from corrosion damage [7].

Another widely-used fluid is the synthetic cutting fluid, which is defined as a water-extendible product free of oil. A combination of alkanolamine and sodium nitrite inhibitor package is used in this type of fluid. Therefore, this fluid can deliver superb properties in cooling, rust protection, hard-water compatibility and biological resistance [8]. Some other alternatives are also tested based on the concerns of healthy and environmental issues.

d) Chip Removal

The fourth major function of cutting fluid in machining process is to remove chips from the cutting zone. And the fluid will also prevent the machined surface from being scratched by chips. This action is especially useful when dealing with operations like deep-hole drilling, in which the cutting fluid is used under pressure and is fed through the cutting tool to force the chips out of the hole. Proper selection of cutting fluid is still important to avoid excessive foam generation that will interrupt with the machining process [8].

Table 1 summarizes the advantages and disadvantages of each type of cutting fluid for these four basic functions based on a good (G)-moderate (M)-poor (P) criterion.

Table 1: Pros and cons of each type of cutting fluid

	Cooling	Lubrication	Corrosion Protection	Chip Removal
Straight oils	P	G	G	M
Soluble oils	M	G	M	M
Synthetic fluids	G	M	G	M
Semi-synthetic fluids	G	G	G	M

3.3. Delivery Methods

There are several methods available for use to deliver cutting fluids on the cutting area during process machining. Three major application strategies are commonly used. They are manual application, flood application and mist application [9].

The first strategy is manual application. It is often used for some very light duties like small jobs or for hobbyists. The cutting fluid will be applied directly through the cutting zone by the operator. The advantage of this method could be inexpensive and easy to apply. However, there are bunch of disadvantages including intermittent application of fluid which we would like to avoid, poor chip removal capability and limited access to cutting zone since the operator can only brush the cutting fluid on the surface of the workpiece. Thus, the use of manual application of cutting fluid is very limited nowadays.

The second strategy, which is the most common, is flood application. Compared with manual application, it is much more advantageous in terms of continuity of flow, efficiency of chip removal and accessibility to cutting zone. Instead of manual application by operator, a pump will deliver the cutting fluid from storage system to some in-machine piping system and finally penetrate to the cutting zone through a nozzle. Thus the cost of this application would be higher than manual but always reasonable for factory manufacturing. For different operations, various configurations and flow rates will be applied for optimized performance. For example, for turning operation, the flow rate could be 5 gallon per minute; but for screw machining, the flow rate could range from 35 to 60 gallon per minute based on the intensity of work. Frequently, two nozzles will be used in one operation: one is flooding the fluid on the workpiece surface and the other would be used to remove the chips and auxiliary cooling. For the shape of the nozzle, the round one would be capable for most common machining and some fan-shaped nozzles will be used for wider cutters.

The third strategy is mist application, which is best suited for high speed cutting while cutting area is small. It can be an alternative method when flood application is impractical. The disadvantage of mist application is the possibility of inhalation of the mist by the operators. Thus good ventilation system is required to avoid this damage happening. Two types of mist generators are used: one is the aspirator type and the other is direct-pressure type. Other special application methods including chilled cutting fluid and highly pressurized bottled gas are also proved to be effective for some specific occasions. However, the cost of these applications is a big constraint which limits their use in machining industry.

Numerous experiment evaluations have pointed out that it depends on the specific machining operation that what type of delivery methods should be chosen. Traditionally, it is ideal for most metal cutting applications to apply high-pressure and high-volume cutting fluids to force a stream directly into the tool/workpiece and tool/chip interface [10]. However, it cannot be always true. In the next chapter, a specific operation - thin wall machining will be focused on and some problems related to cutting fluids will be discussed.

The infrastructure of the delivery system is also very important to know. The delivery system connects the storage system and the workpiece. It delivers cutting fluids through a pump, a piping system and nozzles. Cutting fluid can be delivered to workpiece through flood or mist application. For a flood application, fluid is directed under pressure to the workpiece interface in a manner that produces maximum results. Pressure, direction and shape of the stream are critical for an optimized performance. For a mist application, fluids are atomized and blown onto the workpiece in form of mist. The pressure and direction of the stream are also crucial to the success of the application.

The pump is used to get coolant from a sump to the machine. It is always mounted at the side of the machine for an individual storage system or integrated in the central reservoir system. A motor is usually accompanied to actuate the pump to work. Figure 4 shows a typical structure of the pump system of Haas Mill Drill Center that is used at WPI Washburn Shop.

It is also very critical to acquire the specifications of the pump for machine tool. It reflects the capability of the pump for delivering the cutting fluid to the cutting space. This capability varies from pump to pump. Common pumps used with daily CNC machines are always centrifugal ones. A centrifugal pump can consume 3-5 horsepower and is capable to reach a maximum pressure to 200 psi (approximately 1380 kPa). This pressure can be adjusted by turning the valves either on the pump or on the piping system. Thus it can be recognized that the pressure force delivered to the cutting area can be very large [10].

Figure 4: Coolant pump for Haas Mill Drill Center

A flexible coolant pipe as shown in Figure 5 is widely used in cutting fluid system. Its length and angle can be adjusted easily without affecting the performance of the coolant. It is usually made of PVC, nylon, Delrin, etc. The diameter of a common round coolant nozzle is approximately 1 inch (25.4 mm).

Figure 5: Flexible coolant pipe with a nozzle

A nozzle can be either round or flat in terms of shape. Nozzles in different shapes can deliver various types of stream of cutting fluid, such as lamina flow or vortex flow. It can also be categorized into traditional and programmable one. For a traditional nozzle, the angle and direction can only be adjusted by hand. For a programmable nozzle, the position and the pressure can be controlled via a program. In some modern CNC, it has been a standard feature as shown in Figure 6. Such kind of programmable nozzle makes the precise tuning of the nozzle angle possible and can be easily controlled during machining process. Some machine controllers can even store the nozzle position for each tool.

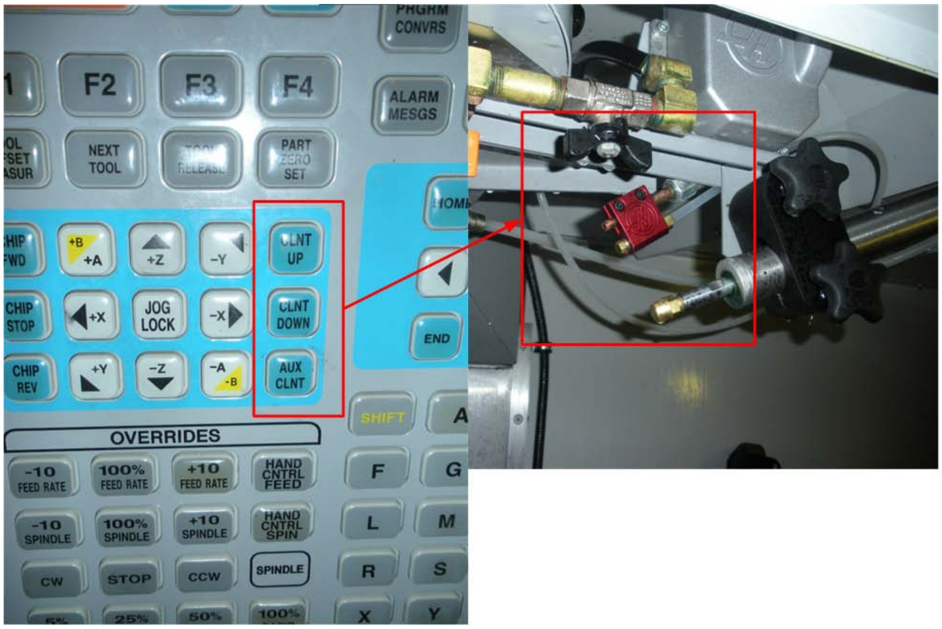

Figure 6: Programmable nozzle

It is also noticed that not only the angular position of the nozzles matters for the performance of cutting fluids during the machining processes, but also the installed position where altitude can be a factor that influences the performance. Figure 7 shows the nozzles installed in Haas Mill Drill Center located at Worcester Polytechnic Institute, Washburn Shops. From the picture, it can be observed that there is an extremely long distance (approximately 10-15 inches) between the nozzle and cutting area. This could make the delivery of the cutting fluid inconsistent and finally result in an unstable machining.

Figure 7: Installment of the nozzles in Haas Mill Drill Center

3.4. Other Related Issues of Cutting Fluid

Besides the functional roles and delivery methods, there are some other related issues about cutting fluid, including storage, recycling, disposal and failure modes. Each of these issues can impact on the machining process. These impacts will not have been studied in this thesis, but can be a good direction for the studies in the future.

a) Storage

The proper storage of cutting fluids is of great importance to prevent contamination and deterioration. Some recommendations are given as follows for guiding the proper storage of cutting fluids [11].

- Storing of fluid in clean seal-able drums clearly marked, protected from frost or sunlight and preferably indoor;
- Have adequate ventilation and fire extinguishers in the storage area;
- Clean up spills with inert, mineral absorbent materials;
- Keep strong oxidizing agents out of the storage area;
- Do not use sawdust or oily cotton waste for spill control.

The storage sump for cutting fluids can be either placed with machine tool or separately. For small work shop, the former is always applied due to its low cost and easy setup. However, it is believed that for higher level applications, a central cutting fluid storage system takes more advantages. Within such a system, the cutting fluid is stored in one place and shared by several machine tools. The disadvantage is lack of flexibility of the system. Since one system can often handle with one kind of cutting fluid at one time, it may be difficult for dealing with various kinds of machining jobs.

Inappropriate storage of cutting fluids could result in some problems including tramp oils, particle contaminants or bacteria and fungi generation. Figure 8 shows the storage sump for Haas Mill Drill Center located at Worcester Polytechnic Institute, Washburn Shops. It can be seen from the figure that if the coolant sump or tank is not well sealed and exposed to the outside environment for a long time after use, the problems mentioned above truly exist there and it is believed that it could lead to potential machining problems.

Figure 8: Contaminants in coolant sump

b) Recycling

The quality of the cutting fluid will eventually reach a point that routine maintenance is no longer effective. Then, it needs to be recycled or even disposed. To recycle the fluid, the critical aspect is to recycle it at right time. The cutting fluid will become not suitable for recycling if it degrades over the limit [12]. That is why monitoring the quality and performance of cutting fluid is of great importance in fluid management.

The conventional equipment for recycling is listed in Table 2.

Table 2: Conventional contaminant removal equipment

Equipment	*Contaminant Removed*
Skimmers	Tramp Oil
Coalescers	Tramp Oil, Particulates
Flotation	Tramp Oil, Particulates
Settling Tanks	Particulates
Magnetic Separators	Particulates
Hydrocyclones	Particulates
Filtration Equipment	Particulates
Centrifuges	Tramp Oil, Particulates, Bacteria

Basically, the frequency for recycling the cutting fluid depends on the life expectancy of the fluid itself. If the cutting fluid is required to be disposed after two or three months, it should be treated monthly or if it is disposed only after two or three weeks, it should be treated weekly. Typically, the contaminated fluid is sucked out of the individual sump of each machine and placed in a batch-treatment recycling unit for contaminant removal.

Some built-in recycling systems have already been deployed in modern CNC machines. However, the impacts of these systems are limited due to the cost or other issues. Figure 9 shows part of the recycling system in Haas Vertical Machining Center VF-4SS located at Worcester Polytechnic Institute, Washburn Shops. The screw mechanism in the picture is used to move out the chips away with the cutting fluids. Some invisible filtration equipments are installed between this mechanism and the sump at the bottom of the machine. However, by observing the sump after a long period machining time, it is found that there are still contaminants such as tramp oils and micro chips in the sump floating above the cutting fluid.

Figure 9: Recycling mechanism in Haas VF-4SS

c) Disposal

Even with the best recycling system, the cutting fluid will eventually deteriorate and require being disposed. Due to extremely strict regulations by Federal and State environment and health agencies, it is increasingly difficult to dispose the waste fluids. It is required by regulations that the generator of the waste fluids is responsible for determining whether the fluid is nonhazardous or hazardous. The cost for disposing the waste fluid can range from 25 to 50 cents per gallon for nonhazardous waste up to hundreds of dollars per drum for hazardous waste [4]. If the waste fluid is determined to be hazardous, it must be disposed in EPA-certified treatment facilities while if it is nonhazardous, it can be disposed in different ways such as being hauled to a treatment facility, following permission from local wastewater treatment authorities or discharged to a municipal sanitary sewer system.

The fluid should be disposed instead of recycling if any of the following happens:

- pH value is less than 8.0 while the normal range should be 8.5 to 9.4;
- Fluid concentration is less than 2.0% while the normal range should be 3.0% to 12.0%;
- Appearance is dark grey to black while the normal range should be milky white;
- Odor is strongly rancid or sour while the normal is a mild chemical smell.

Based on the current methods to recycle and dispose the cutting fluids and some investigations in local manufacturing companies, it is concluded that it really costs a lot of money to deal with the used cutting fluid, either to recycle or to dispose. According to these concerns, we propose to establish a real-time monitoring system for the performance of the cutting fluid in machining process. Such a system should be capable to monitor the impact of cutting fluid on the machining process and make adjusts according to the machining deviation automatically or give warnings to the machine operator. Figure 10 shows a schematic structure of such a system. It is ideal to be a closed-loop system which is able to self control with less human input. Also the storage section of such a system should be more flexible than the current storage sump. Since it is ideal for the storage drums to be sealed from the manufacturer to the machine tool all the time, an interchangeable storage section could be constructed to make sure that the cutting fluid will not be contaminated before reaching the cutting area. And the other advantage of such a storage system could be that it can handle with different types of cutting fluid easily and simultaneously by just switching on and off among several valves. And more efficient filtration section should also be considered in such a system. Various types of filtration equipment should be deployed for different sources of contaminants. The purpose is to make sure that the cutting fluid is cleaned as much as possible before returning to the storage section.

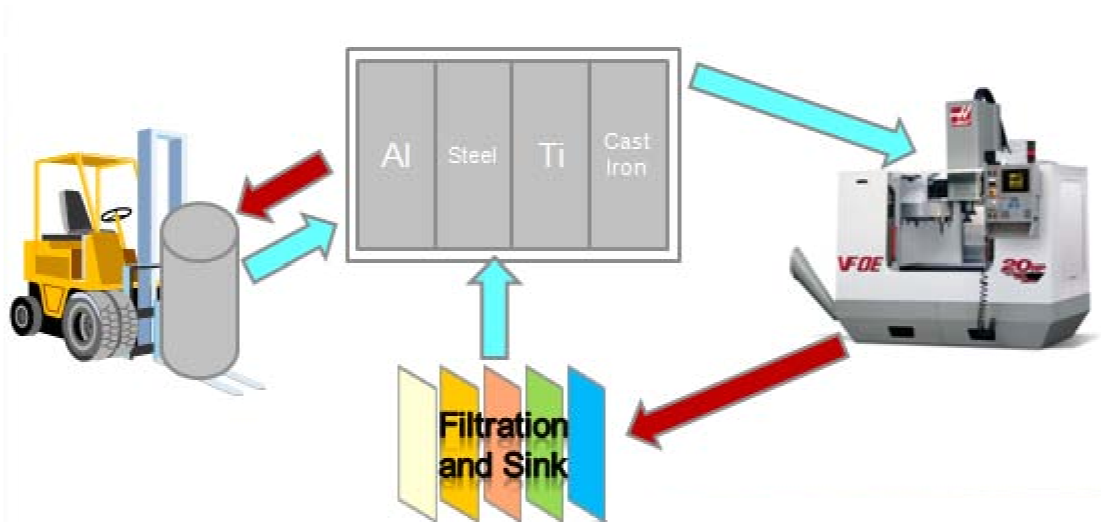

Figure 10: A schematic system for all-in-one solution of cutting fluid

d) Failure Modes

If the cutting fluid is not dealt with in a proper way in terms of one or more aspects mentioned above, the machining process might fail in different ways. Table 3 is a summary of failure modes and their causes and solutions [13].

Table 3: List of failure modes

Failure Mode	*Causes*	*Solutions*
Foaming	Concentration too high	Adjust concentration
	Machine cleaner in sump	Check pH Allow machine to run, cleaner should dissipate
	Mechanical	Check machinery and repair as required
	Soft water	Sample water, treat it necessary
	High tramp oil content	Skim off oil Check hydraulic lines for leaks and repair as required
Rusting	Concentration too low	Adjust concentration
	Poor mixing	Add concentrate to water
	High tramp oil content	Skim off oil Check hydraulic lines for leaks and repair as required
Poor Tool Life	Concentration too low	Adjust concentration
	Wrong product being used	Look up for right products
	Large amounts of biocide added to sump or system	Refer to operation manual for right amounts
	High tramp oil content	Skim off oil Check hydraulic lines for leaks and repair as required
Odor	Low concentration	Adjust concentration
	Low pH	Check pH
	High tramp oil content	Skim off oil Check hydraulic lines for leaks and repair as required
	Contamination	Sample and look for further

		assistance from agents
Skin Irritation	High concentration	Adjust concentration
	High pH	Check pH
	High tramp oil content	Skim off oil Check hydraulic lines for leaks and repair as required
	Dirty shop clothes	Use only clean cloths
	Allergies	Have operators checked for allergies
	Out-of-shop influences	Check pH
Residue in Machine	High concentration	Adjust concentration
	High tramp oil content	Skim off oil Check hydraulic lines for leaks and repair as required
	Incorrect mixing	Refer to operation manual
	High misting operations	Check ventilation system Adjust coolant nozzles

Here are some common solutions for otential failure modes that could happen when applying cutting fluids. Future studies may focus on building an intelligent expert system with a knowledge library to help workshops to identify the cutting fluid problems and provide proper solutions. Besides, more failure modes can be added to this knowledge library, such as my following analysis.

In the next chapter, previous studies on evaluating the performance of cutting fluids during machining processes will be reviewed. And since the specific milling operation will be selected as the object we are going to model on for our own analysis, the classical milling processes will also be reviewed, especially on thin wall machining.

Chapter 4. Performance Evaluation of Cutting Fluids

4.1. Previous Studies

Numerous preceding papers and works have been brought up to study the performance evaluation of cutting fluids. Most of them focus on the impact brought by cutting fluids on machining processes in terms of the type of the cutting fluid, the delivery methods and different machining operations. Some of these studies are to try to find some direct correlation between some aspects of cutting fluids and machining performance. While some are to make efforts to establish some evaluation criteria to assist the selection and application of cutting fluids in machining processes.

Axinte et al. [39] discussed effectiveness and resolution of five cutting tests including turning, milling, drilling, tapping and VIPER grinding and their quality output measures used in a multi-task procedure for evaluating the performance of cutting fluids when machining aerospace materials. The resolution given by experimental data was evaluated and a comparison of robustness in ranking the performance of cutting fluids based on different output measures and cutting tests was presented.

Sales et al. [40] demonstrated some scratch test techniques which can be used to provide a quick and cost effective evaluation of cutting fluids. Apparent coefficient of friction and specific energy for the scratch steel samples under several lubrication conditions provided a good indicator of cutting fluid performance which was followed by evaluation of the surface finish and the cutting force of the ABNT NB 8640 steel with emulsion and synthetic cutting fluids, at 5% of concentrations, and mineral oil in the turning process. Comparative tests were carried out under dry and wet conditions. Results showed that the linear scratch test was not efficient while the scratch test was efficient tool in the classification of cutting fluids.

Axinte et al. [41] also described the results of a comprehensive evaluation program for cutting fluid efficiency when machining the aerospace alloy Inconel 718. The machining methods included milling, drilling, tapping and VIPER grinding, Results from three cutting fluids including semi-synthetic fluids, synthetic fluids and emulsified oils were. Cutting forces, torque and spindle power were acquired during machining. Geometry accuracy surface texture and surface integrity of the workpiece were analyzed. The experimental results demonstrated the difficulty for identifying the best cutting fluid, especially when several different machining methods are employed on the machine tool. It was unlikely that a single fluid could show the best performance on all machining trials. Therefore, they established a multi-criteria model to assess the performance of cutting fluids according to the time schedule for the customer. This methodology based on various tests was proved to be able to evaluate the effectiveness of cutting fluid very comprehensively.

Although amounts of studies have been performed previously, almost all of these studies are based on the experimental results without mathematical modeling and analysis. Very few of them focus on the dynamic impacts of cutting fluid on the machining processes, especially the machining stability. This thesis attempts to establish a correlation between the penetration force of cutting fluid and machining stability..

Based on the author’s own machining experience, this thesis is going to focus on milling operations and thin wall. Thus in the following sections, general knowledge of milling operations and thin wall machining is reviewed for the modeling analysis in the next chapter.

4.2. Review on Milling Operations

Milling is the most widely used machining process the cutting tool carries out a rotary motion and the workpiece is fed in a linear motion during milling. It is mostly used for machining flat surfaces, slots and contoured features. Unlike turning, milling is always a multi-point cutting process using face milling cutters or end mills. Generally speaking, milling can be classified into two types based on different orientations of spindle: one is horizontal milling and the other is vertical milling [14].

The characteristics of horizontal milling include:

- The cutting teeth are arranged on the surface of the cylindrical tool;
- There is a contact between the cylindrical surface of the cutter and the machined surfaces;
- The machined surface is parallel to the cutter’s axis of rotation.

The characteristics of vertical milling include:

- The cutting edges are situated both on the face of the end mill and on its cylindrical surface;
- There is a contact between the face of the milling cutter and the machined surfaces;
- The machined surface is generated at right angle to the cutter axis of rotation.

Milling operation can also be classified into two types based on the rotary direction of the spindle with respect to the feed direction of the workpiece. They are conventional milling and climb milling [14].

In conventional milling, the feed direction of workpiece is opposite to the direction of the milling cutter. In climb milling, the feed direction of workpiece is in the direction of the milling cutter.

The advantages of conventional milling include:

- It is safer in operation due to the separating forces between the cutter and workpiece;
- Fragments of built-up edge are absent from the machined surfaces;
- The tool life is not affected by the sandy surfaces;
- Working loads are not applied suddenly at the teeth;
- Looseness in moving parts does not damage the cutting motion.

The advantages of climb milling include:

- It is possible to use simplified fixtures to mill parts that cannot be easily held on the table;
- Machined surface are not affected by the revolution marks and easily polished;
- It requires lower machining power;
- The tendency of vibrations is low;
- There is less tool wear on the cutting edge;

- It provides favorable cutting conditions that lead to better surface finish.

Generally speaking, climb milling is much preferred in today's machining practice. It can provide favorable cutting conditions such as lower cutting forces and less tool wear which lead to better surface quality. Because the cutter is always tending to climb on the workpiece, climb milling requires much stiffer equipment such as machine tool and fixtures without looseness in the feeding mechanism. Along with the spreading use of CNC machining center and other rigid machine tools, climb milling has been applied over 99% out of all the milling processes in industry nowadays.

Figure 11 presents the difference between conventional milling and climb milling.

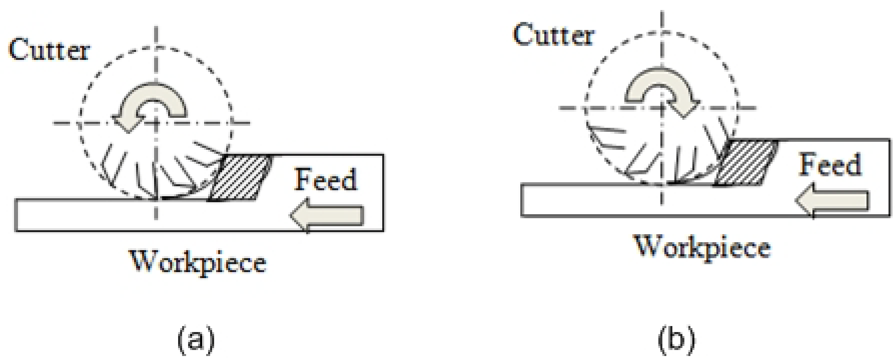

Figure 11: (a) Conventional milling vs. (b) Climb milling

No matter what type of milling it is, the cutting forces involved in milling operation are tangential force perpendicular to the cutter radius and normal force along the radius. The directions of the cutting forces are different depending on the type of milling.

The resolution of forces in conventional milling and climb milling are shown in Figure 12.

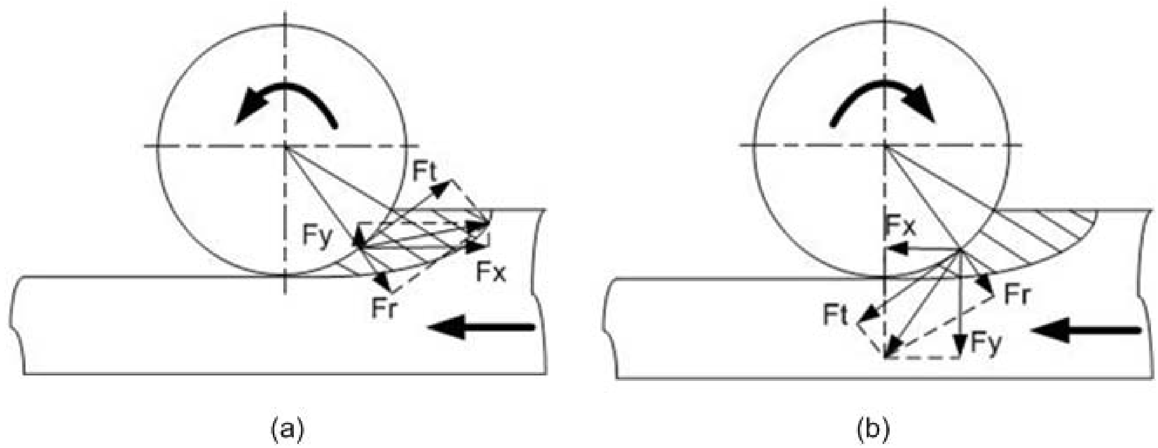

Figure 12: Cutting forces resolutions in (a) Conventional milling and (b) Climb milling

Cutting forces are widely recognized as an optimum performance estimator of machining operations [15]. Large cutting forces are result of the extreme conditions at the tool-workpiece interface. This interaction can be directly related to the tool wear and, in the worst of the cases, lead to failure of the tool [16]. Consequently, tool wear and cutting forces are related, although that relationship is different for each different wear mechanism shown in Figure 13 (flank, crater, tool breakage).

Figure 13: Tool wear on end mill

Cutting forces are also related with chatter and process instability [17-18]. Chatter results in a loss of accuracy of machined parts or in damages of the machines structure. The unexpected variations of the cutting forces can be responsible for the damage of the ceramic hybrid bearings of the high-speed spindle, which means an important time and money waste during repairs. The study of this situation will be easier if cutting forces were recorded according with the part geometry. Finally, the machine and tool deformations due to cutting forces affect the surface finish and the dimensions of machined parts.

Cutting forces in milling operations can be measured in different ways. One way is to monitor the power consumed and calculate the forces based on the classical model mentioned above. The other way is to directly monitor the forces on each axis by deploying the dynamometer. Figure 14 shows a schematic representation for measuring forces using dynamometer and computer.

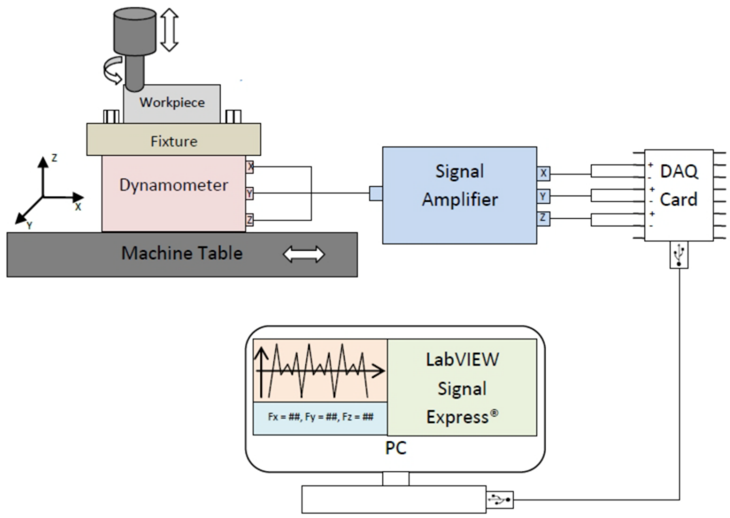

Figure 14: Measuring the cutting forces in milling

4.3. Thin Wall Machining

At present, thin walls are commonly applied in machining aeronautical and aerospace components. Figure 15 shows some applications such as torpedoes and airplane wings manufactured as thin wall machining. Thin wall parts contribute a lot to decrease the weight of these products which have strict requirement for weight or corrosion protection.

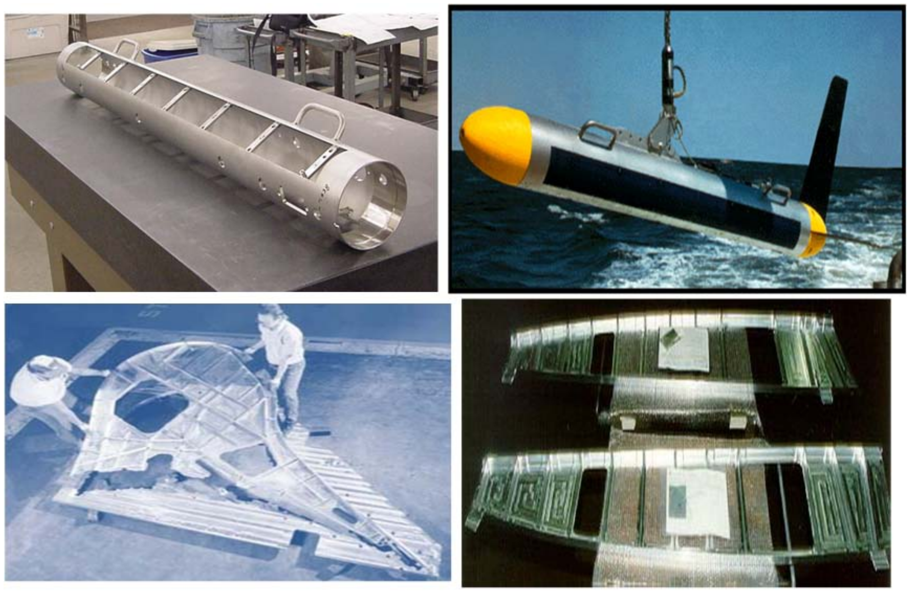

Figure 15: Applications of thin wall machining

Trial machining of thin wall parts have been done regularly at Worcester Polytechnic Institute, Washburn Shops as lab contents for computer-aided manufacturing class. During the labs, parts in different geometries shown in Figure 16 were machined at various cutting conditions. Based on the machining experience and results, it was found that machining in high speed would yield a good result while the machining stability could not be guaranteed always. A fixture for machining thin wall parts was also applied to improve the stiffness of the workpiece as to try to decrease the machining chatters as shown in Figure 17.

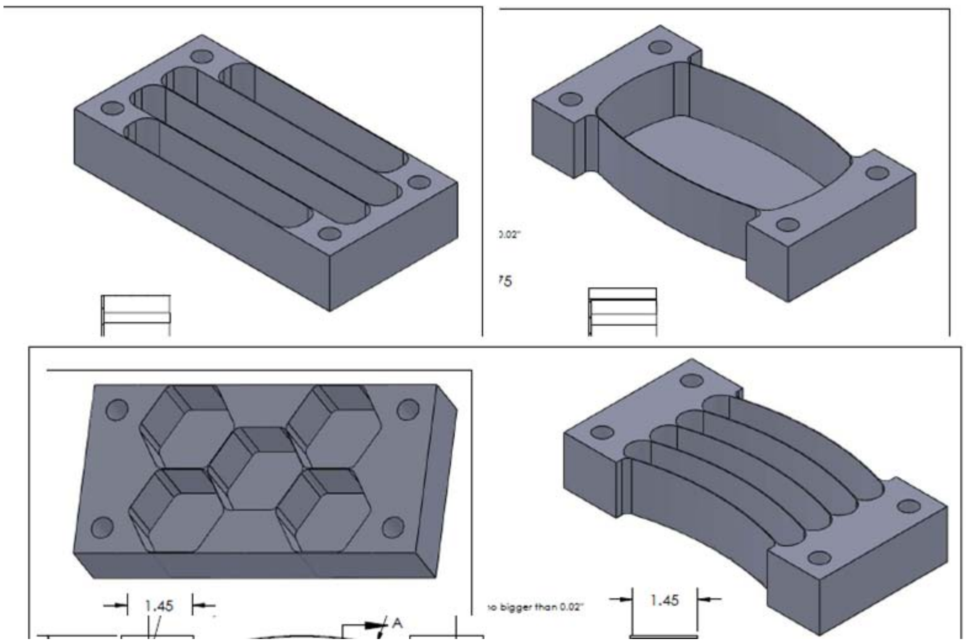

Figure 16: Thin wall machining instants

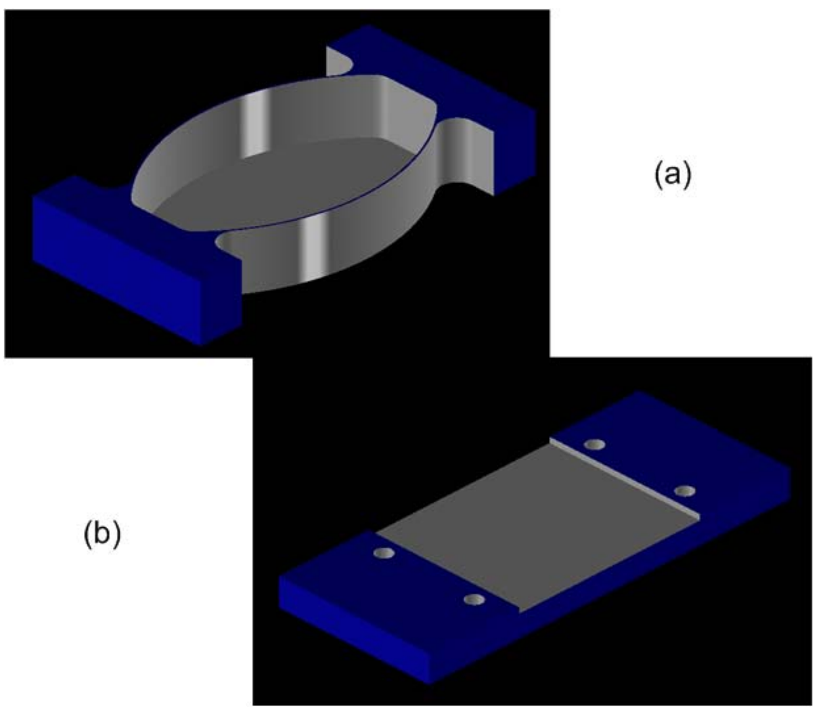

Figure 17: (a) Thin wall part (b) Dedicated fixture for machining thin wall parts

Due to its very low stiffness, thin walls are difficult to machine. Wall deflection or forced vibration and regenerative chatter can easily reduce the quality of thin wall machining. These problems were studied by Smith and Dvorak [19]. They indicated that one major limitation to the widespread use of high speed machining for the production of thin components is the stability of the machining operation. As the wall becomes thinner, it loses stiffness, and consequently, chatter will become more problematic. Such kind of chatter during machining can result in poor surface quality, or even cutting through the thin wall.

Some problems have been pointed out on thin wall machining from previous research. The first problem is caused by the wall static deformation produced by the cutting forces that generate an excess of uncut material. Wall deformation reduces the tool immersion into the wall, and therefore, cutting forces decrease. As the operation approaches the lower part of the wall, the stiffness becomes higher, and so the deformation is smaller and the tool engagement is higher. It can result in an increase of the cutting forces.

The second problem is caused by the machining dynamics. It is especially important when the natural frequency of the wall is close to the teeth passing frequency. It must be taken into account that the natural frequencies of a wall is continuously decreasing during milling due to the progressive reduction of both the mass and stiffness of the wall.

The third problem is caused by self-excited vibration, which is the cutting process itself that generates oscillations. The origin of these oscillations, or chatter, is the dynamic excitation produced by the wavy irregular part surface generated by precedent tool tooth. This phenomenon is difficult to detect because the natural frequency of walls changes during machining.

Lopez de Lacalle et al. [15] also indicated that these three types of problems may happen at the same time. It can make it difficult to determine what the true origin of those irregular marks that appears on a milled thin wall. However, besides these three problems mentioned above, no one has considered about the impact of cutting fluid during machining thin walls. Because of the application of high speed machining, it would generate a relatively large amount of heat. And for soft materials like aluminum, the chips are very adhesive to generate built-up edges and require to be flushed away instantly during machining. Thus the use of cutting fluid is necessary in thin wall machining. Therefore, the following analysis in the next chapter will focus on the impact that is brought by the factor of cutting fluid on the machining stability.

Chapter 5. Mathematical Modeling of Milling Chatter and Cutting Fluid

5.1. Establishment of the Mathematical Model

The single degree of freedom model describing the correlation between the penetration force of cutting fluid and regenerative chatter milling is governed by the delay differential equation:

$$m\ddot{x}(t) + c\dot{x}(t) + kx(t) \qquad (1)$$
$$= \Delta f_x\left(\alpha_j(t), \Delta h_{j\kappa}\left(s_{j\kappa}, \alpha_j(t)\right), \mu_1\right) + \Delta g_{cx}\left(\alpha_j(t), \dot{m}\left(\alpha_j(t), \dot{\vartheta}_l(t)\right), \mu_2\right)$$

where m is the mass of the milling cutter, c and k are the viscous damping and stiffness coefficients, respectively. The function $\Delta f_x\left(\alpha_j(t), \Delta h_{j\kappa}\left(s_{j\kappa}, \alpha_j(t)\right), \mu_1\right)$ is the change in cutting force along the x-direction and it is dependent upon the angular position $\alpha_j(t)$ of the milling cutter of j-tooth at a specific time t, the variation of the feed $\Delta h_{j\kappa}\left(s_{j\kappa}, \alpha_j(t)\right)$ per j-tooth generating s_{jk}-chip segments, and the parameter μ_1. The parameter μ_1 represents the product of the width of cut w and the ratio of the regenerative cutting force k_1 and stiffness k of cutter model. For $\kappa \leq j = 1,2,3, \cdots n$ and n being a real integer, we let z_j to denote the total number of teeth in the cutter and z_{jc} to represent the number of j-tooth of the milling cutter that are simultaneously in contact with the workpiece. The regenerative time, denoted by τ_1 is defined as $\tau_1 = 2\pi/\left(z_{jc}\Omega\right)$ where Ω is spindle speed of the milling cutter in revolution per minute. Furthermore, let $\alpha_{j,ent}(t)$ and $\alpha_{j,exit}(t)$

denote the entering angular position of the milling cutter of the j -tooth at $h_{j\kappa}\left(s_{j\kappa},\alpha_j(t)\right)_{min}$ and exiting angular position at chip thickness $h_{j\kappa}\left(s_{j\kappa},\alpha_j(t)\right)_{max}$, respectively. The feed per tooth $h_{j\kappa}\left(s_{j\kappa},\alpha_j(t)\right)$ is described as $h_{j\kappa}\left(s_{j\kappa},\alpha_j(t)\right) = 2\pi r/\left(z_{jc}\Omega\right)$, where r is the feedrate or the feed velocity of the machine tool table. And then the j-tooth of the milling cutter removes material in the form of chips for $z_j = z_{jc}$ when the inequalities $\alpha_{j,ent}(t) \leq \alpha_j(t) \leq \alpha_{j,exit}(t)$ and $h_{j\kappa}\left(s_{j\kappa},\alpha_j(t)\right)_{min} \leq h_{j\kappa}\left(s_{j\kappa},\alpha_j(t)\right) \leq h_{j\kappa}\left(s_{j\kappa},\alpha_j(t)\right)_{max}$ hold. These inequalities, in particular, indicate that machining is attainable, and that there is a continuous engagement between the j-tooth and workpiece.

We make use of the fact that, the engagement may be discontinued at some specific time in the interval $\alpha_{j,ent}(t) \leq \alpha_j(t) \leq \alpha_{j,exit}(t)$ so as to define the milling engagement regime in the interval $\alpha_{j,ent}(t) \leq \alpha_j(t) \leq \alpha_{j,exit}(t)$, namely

$$\chi_{j\kappa}\left(\alpha_j(t), z_{jc}\right) := sign\left(\alpha_j(t), z_{jc}\right) \tag{2}$$
$$= \begin{cases} 1, & h_{j\kappa}\left(s_{j\kappa},\alpha_j(t)\right)_{min} \leq h_{j\kappa}\left(s_{j\kappa},\alpha_j(t)\right) \leq h_{j\kappa}\left(s_{j\kappa},\alpha_j(t)\right)_{max} \\ 0, & h_{j\kappa}\left(s_{j\kappa},\alpha_j(t)\right) > h_{j\kappa}\left(s_{j\kappa},\alpha_j(t)\right)_{max} > h_{j\kappa}\left(s_{j\kappa},\alpha_j(t)\right)_{min} \\ -1, & h_{j\kappa}\left(s_{j\kappa},\alpha_j(t)\right)_{min} < h_{j\kappa}\left(s_{j\kappa},\alpha_j(t)\right) < h_{j\kappa}\left(s_{j\kappa},\alpha_j(t)\right)_{max} \end{cases}$$

where the value of $\chi_{j\kappa}\left(\alpha_j(t), z_{jc}\right) = 1$ indicates that j-tooth of the milling cutter are cutting and for $\chi_{j\kappa}\left(\alpha_j(t), z_{jc}\right) = 0$, they are not cutting. In the interval $\alpha_{j,ent}(t) \leq \alpha_j(t) \leq \alpha_{j,exit}(t)$, interrupted or intermittent nonlinear milling forces may cause a temporary disengagement between the j-teeth of the milling cutter and workpice, and the value of $\chi_{j\kappa}\left(\alpha_j(t), z_{jc}\right) = -1$ represents this aspect.

The angular position $\alpha_j(t)$ of the milling cutter of j-tooth is defined as $\alpha_j(t) = \Omega t + \alpha_j(t_0)$ where $\alpha_j(t_0)$ is the equally spacing angle between adjacent milling teeth on the cutter (see Figure 18) at some specific initial time t_0.

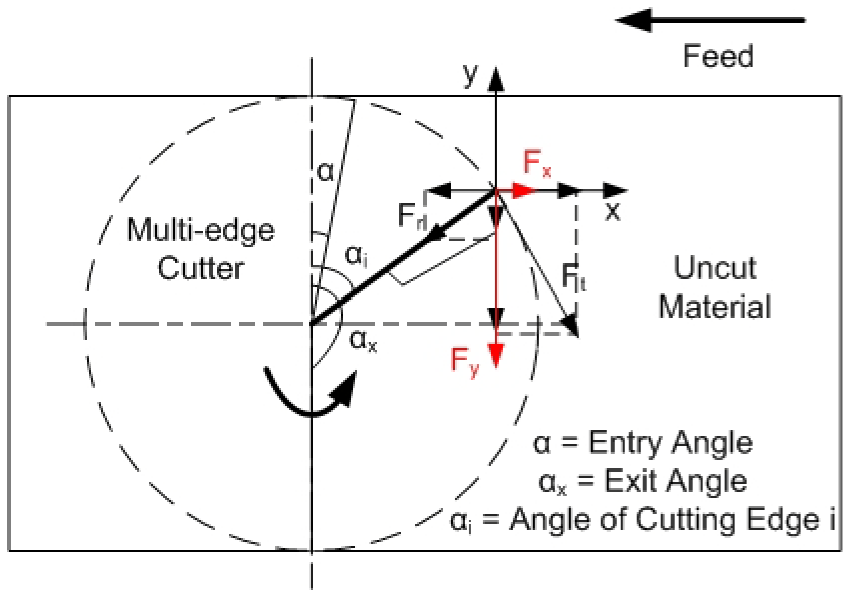

Figure 18: Angular position of cutter engagement

We know that $\alpha_j(t_0) = 2\pi/z_j$ and also $\alpha_j(t_0) = \alpha_j(t)/z_{jc}$, and from these two expressions yield

$$\alpha_j(t_0) = \frac{2\pi z_{jc} + z_j \alpha_j(t)}{z_j z_{jc}} \tag{3a}$$

And hence we define angular position $\alpha_j(t)$ of the milling cutter of j-tooth as

$$\alpha_j(t) = \Omega t + \alpha_j(t_0) = \frac{z_{jc}}{z_{jc} - 1}\left(\Omega t + \frac{2\pi z_{jc}}{z_j}\right) \tag{3b}$$

With the equally spacing angle $\alpha_j(t_0)$, the magnitude of cutting force variation on each j-tooth of the milling cutting will be the same, but for unequal spacing angle $\alpha_j(t_0)$, the impact of cutting force variation on each j-tooth changes. In such a situation we have the angular position $\alpha_j(t)$ of the milling cutter of j-tooth as the form

$$\alpha_j(t) = \frac{z_{jc}}{sign(z_{jc} - z_{jc,min}) - 1}\left(\Omega t + \frac{2\pi z_{jc}}{z_j\, sign(z_{jc} - z_{jc,min})}\right) \tag{4}$$

where $z_{jc,min}$ is the minimum number of j-tooth that are simultaneously in contact with the workpiece at a particular time and maximum number is $z_{jc,max} = z_{jc,min} + sign(z_{jc} - z_{jc,min})$. The contact length of arc of the j-tooth in the interval $\alpha_{j,ent}(t) \leq \alpha_j(t) \leq \alpha_{j,exit}(t)$ is given by $l = \alpha_j(t)\, D/2$ where D is the diameter of the milling cutter. The influence of the cutting fluid on cutting force variation has been one of the most difficult influences to define and quantify. It is difficult to evaluate the influence from knowledge of general practices of applying coolants into machining operations without taking into considerations of the cutting fluid properties, velocities, forces and mass flow rates. Attempt is made below to establish relations for cutting fluid influence.

Before the mathematical analysis, the model that is studied is presented as follow. Figure 19, Figure 20 and Figure 21 show the case that cutting without cutting fluid or we say dry machining which include the operation setups, motion geometry and force resolutions. Figure 22, Figure 23 and Figure 24 indicate the case that cutting fluid impacts on the milling operation as compared with the first case.

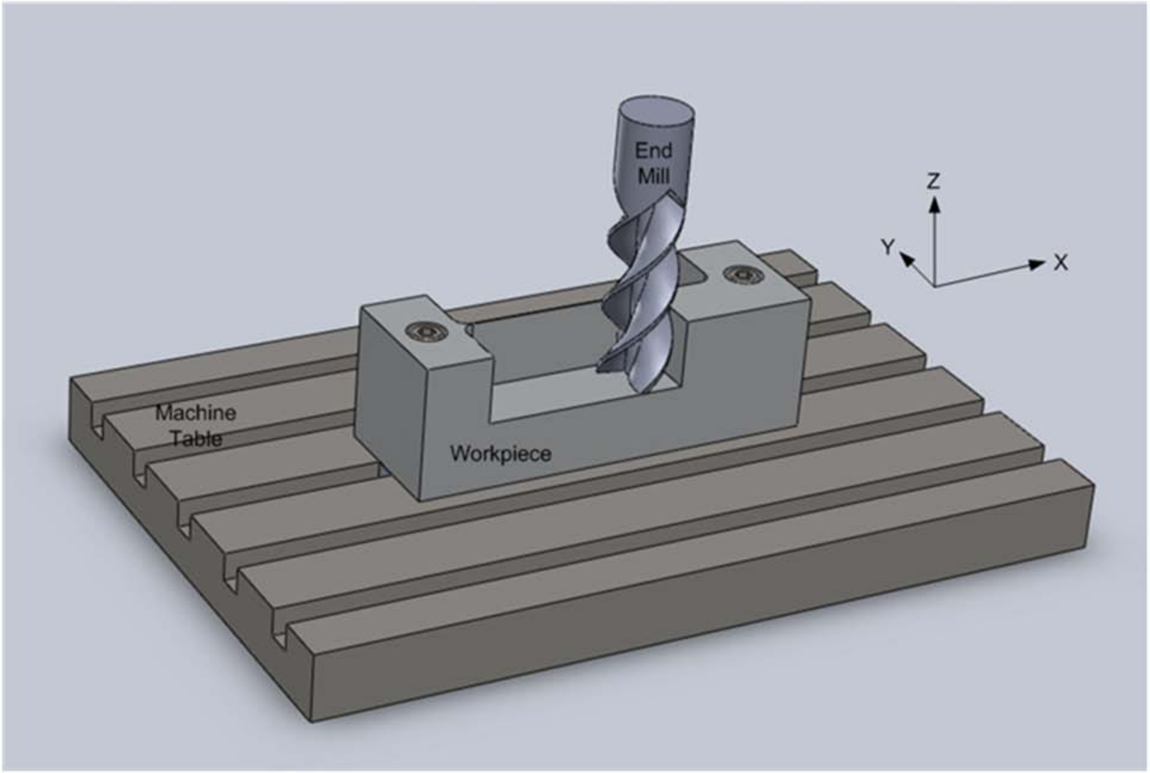

Figure 19: Cutting without cutting fluid - Operation setups

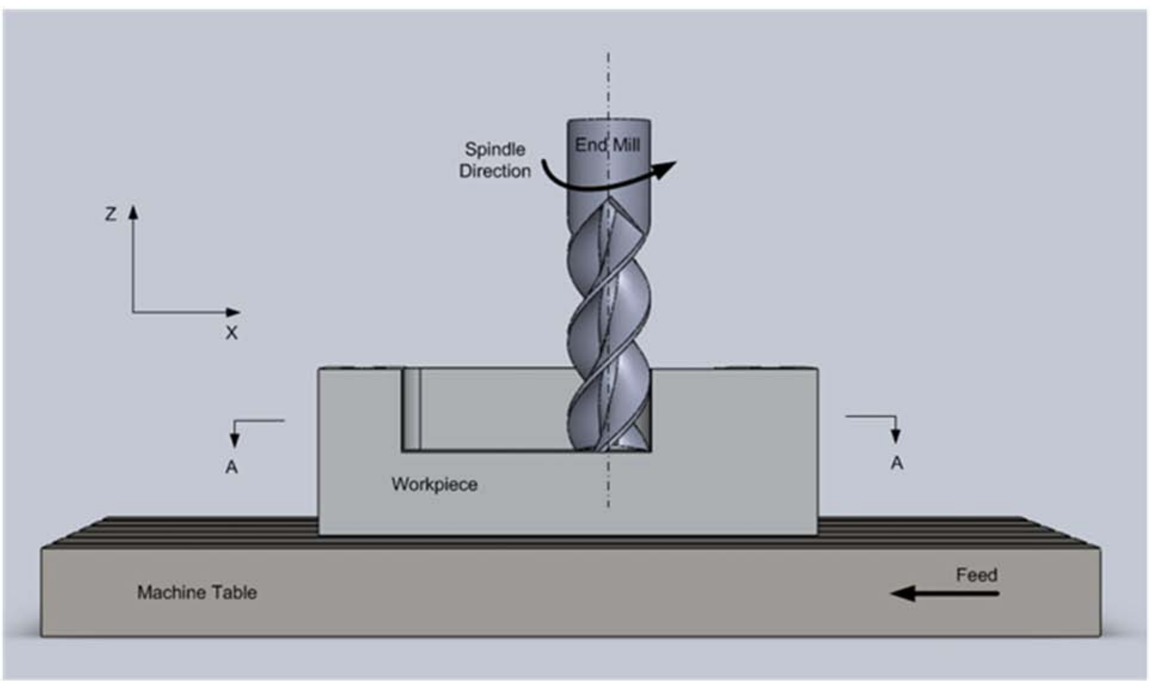

Figure 20: Cutting without cutting fluid - Motion geometry

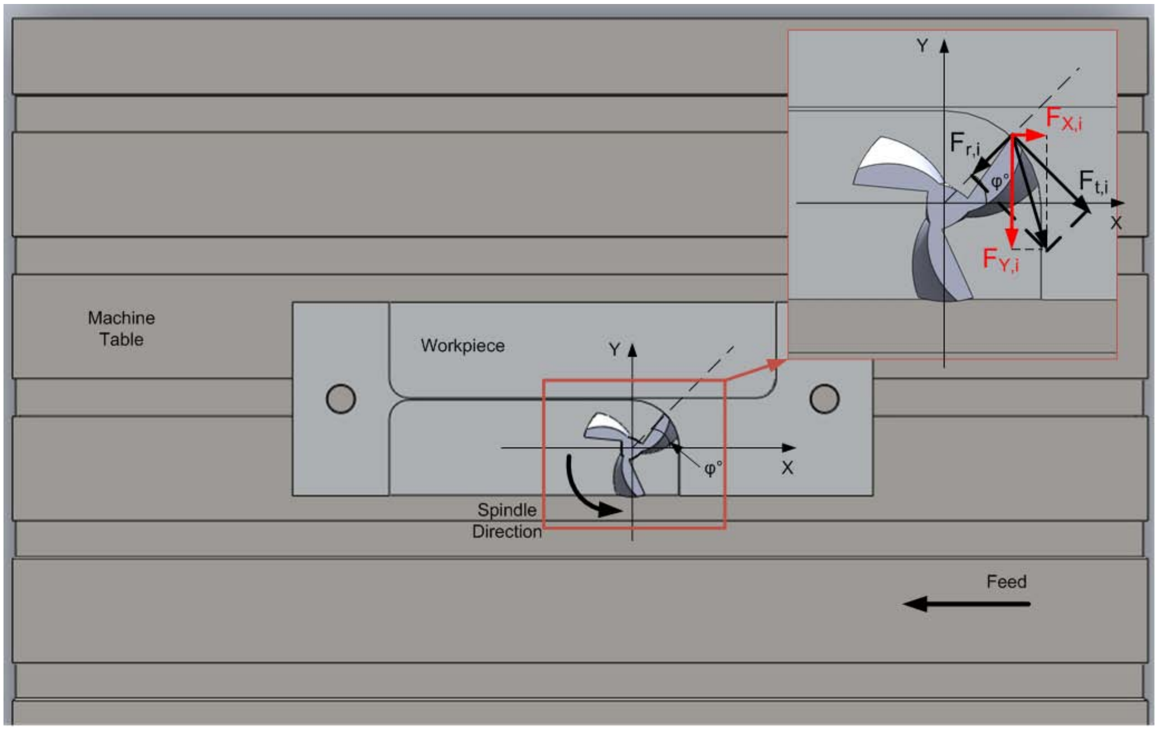

Figure 21: Cutting without cutting fluid - Force components

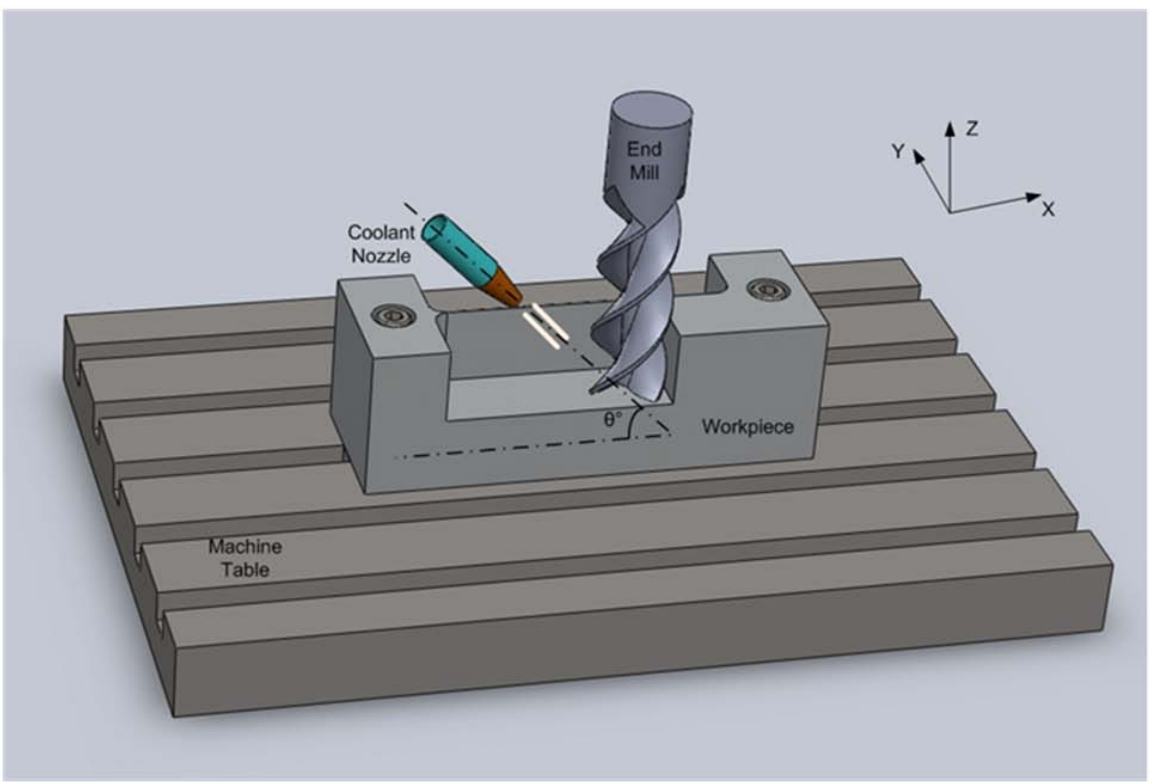

Figure 22: Cutting with cutting fluid - Operation setups

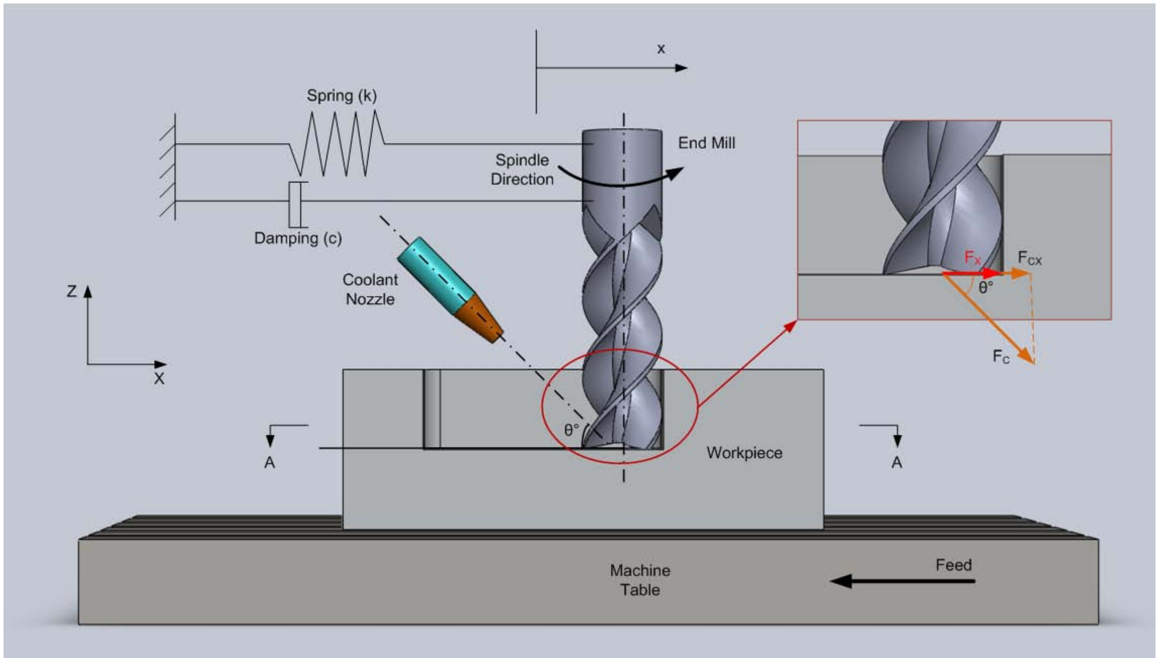

Figure 23: Cutting with cutting fluid - Motion geometry and dynamic model

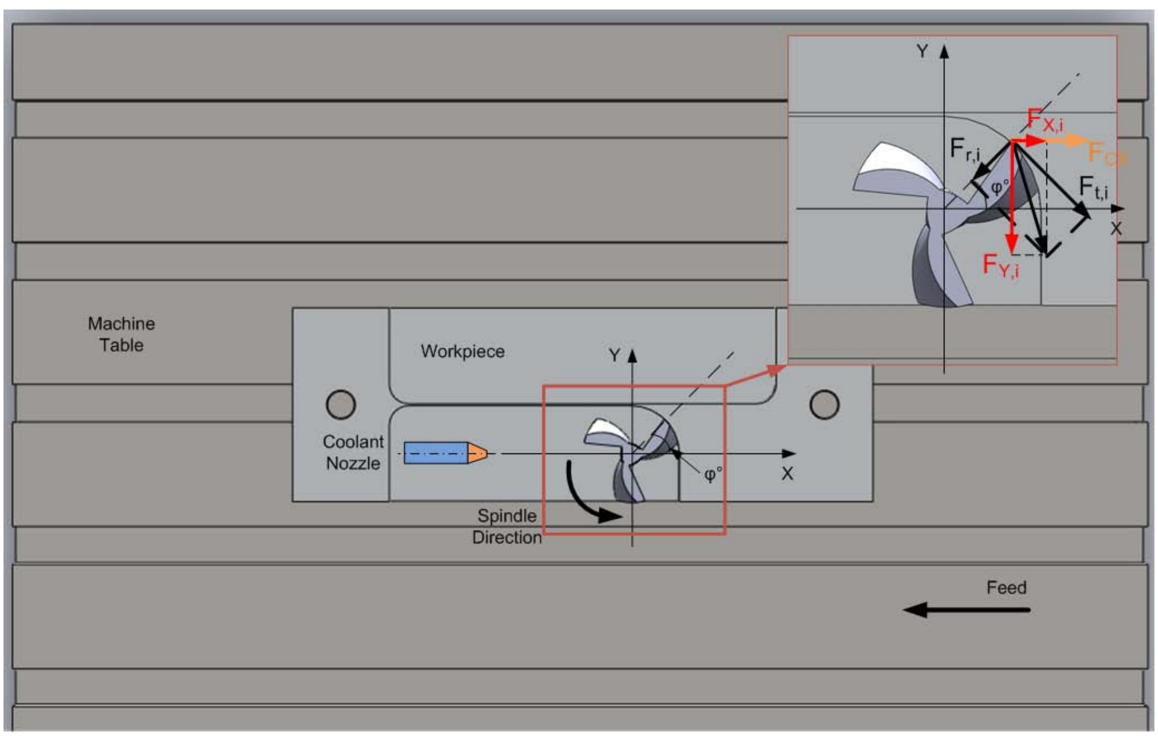

Figure 24: Cutting with cutting fluid - Force components

5.2. The Influence of Cutting Fluid Force on Milling

Determination of the force variation $\Delta g_{cx} = \Delta g_{cx}\left(\alpha_j(t), \dot{m}\left(\alpha_j(t), \dot{\vartheta}_l(t)\right), \mu_2\right)$ of the cutting fluid requires information about the mass flow rate $\dot{m}\left(\alpha_j(t), \dot{\vartheta}_l(t)\right)$ of the cutting fluid into the interval $\alpha_{j,ent}(t) \le \alpha_j(t) \le \alpha_{j,exit}(t)$ of chip thickness $h_{j\kappa}\left(s_{j\kappa}, \alpha_j(t)\right)_{min} \le h_{j\kappa}\left(s_{j\kappa}, \alpha_j(t)\right) \le h_{j\kappa}\left(s_{j\kappa}, \alpha_j(t)\right)_{max}$, namely

$$\dot{m}\left(\alpha_j(t), \dot{\vartheta}_l(t)\right) = \int_{\alpha_{j,ent}(t)}^{\alpha_{j,exit}(t)} \left\{\Im\left(\alpha_j(t), \dot{\vartheta}_l(t)\right) + \Theta_{111}\left(\alpha_j(t), \dot{\vartheta}_l(t)\right) - \Theta_{222}\left(\alpha_j(t), \dot{\vartheta}_l(t)\right)\right\} d\alpha_j(t) \tag{5}$$

where $\Im\left(\alpha_j(t), \dot{\vartheta}_l(t)\right)$ is the mass flow rate that is carried by the milling cutter as it rotates, $\Theta_{111}\left(\alpha_j(t), \dot{\vartheta}_l(t)\right)$ represents the rate at which cutting fluid is flooded into the milling process by ℓ-nozzle placed at some angular position with respect to the location of cutting fluid streamline with coolant angular velocities $\dot{\vartheta}_l(t)$, $\ell = 1,2,3 \cdots n$. $\Theta_{222}\left(\alpha_j(t), \dot{\vartheta}_l(t)\right)$ is the rate of cutting fluid mass that is outside the milling operation. The parameter μ_2 denotes the ratio of the fluid force coefficient $\tilde{k}_1$ and stiffness k of the milling cutter. This is the force with which the cutting fluid penetrates the machining operation. The variation of the chip thickness from $h_{j\kappa}\left(s_{j\kappa}, \alpha_j(t)\right)$ to $\Delta h_{j\kappa}\left(s_{j\kappa}, \alpha_j(t)\right)$ inside the interval $\alpha_{j,ent}(t) \le \alpha_j(t) \le \alpha_{j,exit}(t)$ influences the fluid penetration force and mass flow rate $\dot{m}\left(\alpha_j(t), \dot{\vartheta}_l(t)\right)$. During machining, the cutting fluid moves ahead in a given time instant at a point of least resistance from the chips. Coolants in recirculation stages transport contaminants such as debris, chips and bacteria. Contaminations such as tramps oil or chips would decrease fluid delivery force and mass flow rate because they can clog the orifice diameter of the coolant nozzles. The contaminants will slow down the rate of return of the cutting fluid from the nozzles into the interval $\alpha_{j,ent}(t) \leq \alpha_j(t) \leq \alpha_{j,exit}(t)$ at depth of cut d and chip thickness $h_{j\kappa}\left(s_{j\kappa}, \alpha_j(t)\right)_{min} \leq h_{j\kappa}\left(s_{j\kappa}, \alpha_j(t)\right) \leq h_{j\kappa}\left(s_{j\kappa}, \alpha_j(t)\right)_{max}$. The contaminants may present a hazard to the operator if not properly collected and filtered. Insufficient and or intermittent coolant application in milling operation, in particular, can lead to a situation where the cutting fluid may enter the interval $\alpha_{j,ent}(t) \leq \alpha_j(t) \leq \alpha_{j,exit}(t)$ with stable spindle speeds but can be circulated up to unstable spindle speeds before exiting the interval. One can think of this situation as a change in the penetration force of the coolant and mass flow rate $\dot{m}\left(\alpha_j(t), \dot{\vartheta}_l(t)\right)$ with respect to the combined influence of the chip thickness variation $\Delta h_{j\kappa}\left(s_{j\kappa}, \alpha_j(t)\right)$ and the applied torques on the j-tooth of the milling cutter that arise from the gravitational, damping and stiffness of the coolant and milling forces. Naturally one cannot, in general, determine the quantities of $\Theta_{111}\left(\alpha_j(t), \dot{\vartheta}_l(t)\right)$ and $\Theta_{222}\left(\alpha_j(t), \dot{\vartheta}_l(t)\right)$ because of the very long travel period of the cutting fluid before it reaches its intended storage systems. Large coolant recirculation systems, coolant viscosities and degradations over time, cutting tool geometry, coolant routes and application methods, machining conditions, nozzle diameters and locations, and workpiece materials and shapes determine whether or not there is sufficient mass of coolant to provide adequate cooling and chip clearing capability. The considerations of high performance machining lead times are important in designing a machining process and selecting an appropriate coolant. In this thesis work, a great simplification of the force variation $\Delta g_{cx} = \Delta g_{cx}\left(\alpha_j(t), \dot{m}\left(\alpha_j(t), \dot{\vartheta}_l(t)\right), \mu_2\right)$ of the cutting fluid in the interval $\alpha_{j,ent}(t) \leq \alpha_j(t) \leq \alpha_{j,exit}(t)$ is thus the combined Fourier-Taylor series representations

$$\begin{aligned}
&\Delta g_{cx}\left(\alpha_j(t), \dot{m}\left(\alpha_j(t), \dot{\vartheta}_l(t)\right), \mu_2\right) \\
&\quad = \tilde{w}\tilde{k}_1\left\{x(t) - x\left(t - \tau_l\left(\alpha_j(t), \dot{\vartheta}_l(t)\right)\right)\right\} \\
&\quad + \tilde{w}\tilde{k}_2\left\{x(t) - x\left(t - \tau_l\left(\alpha_j(t), \dot{\vartheta}_l(t)\right)\right)\right\}^2 \\
&\quad + \tilde{w}\tilde{k}_3\left\{x(t) - x\left(t - \tau_l\left(\alpha_j(t), \dot{\vartheta}_l(t)\right)\right)\right\}^3 \\
&\quad + \cdots O\left(\tilde{w}\tilde{k}_5\left\{x(t) - x\left(t - \tau_l\left(\alpha_j(t), \dot{\vartheta}_l(t)\right)\right)\right\}^5\right)
\end{aligned} \tag{6a}$$

where the time-varying cutting fluid delay $\tau_l\left(\alpha_j(t), \dot{\vartheta}_l(t)\right)$ is the cosine and sine waves defined by

$$\begin{cases}
\tau_l\left(\alpha_j(t), \dot{\vartheta}_l(t)\right) = \tau_1 + \varepsilon\gamma_l\left(\alpha_j(t)\right), \qquad 0 \leq \varepsilon \ll 1 \\
\gamma\left(\alpha_j(t)\right) = \sum_{m=0}^{\infty} a_m^{(1)} \cos\omega_m\, \alpha_j(t) + \sum_{m=1}^{\infty} a_m^{(2)} \sin\omega_m\, \alpha_j(t)
\end{cases} \tag{6b}$$

and the Fourier constants $a_m^{(0)}$, $a_m^{(1)}$and $a_m^{(2)}$, namely

$$\begin{cases} a_m^{(0)} = \frac{1}{\Gamma\left(\alpha_j(t), \dot{\vartheta}_l(t)\right)} \cdot \\ \int_0^{\Gamma(\alpha_j(t),\dot{\vartheta}_l(t))} \left(\sum_{m=0}^{\infty} a_m^{(1)} \cos \omega_m \, \alpha_j(t) + \sum_{m=1}^{\infty} a_m^{(2)} \sin \omega_m \, \alpha_j(t) \right) d\alpha_j(t) \\ a_m^{(1)} = \frac{1}{\Gamma\left(\alpha_j(t), \dot{\vartheta}_l(t)\right)} \cdot \\ \int_0^{\Gamma(\alpha_j(t),\dot{\vartheta}_l(t))} \left(\sum_{m=0}^{\infty} a_m^{(1)} \cos \omega_m \, \alpha_j(t) + \sum_{m=1}^{\infty} a_m^{(2)} \sin \omega_m \, \alpha_j(t) \right) \cos \omega_m \, \alpha_j(t) dt \\ a_m^{(2)} = \frac{1}{\Gamma\left(\alpha_j(t), \dot{\vartheta}_l(t)\right)} \cdot \\ \int_0^{\Gamma(\alpha_j(t),\dot{\vartheta}_l(t))} \left(\sum_{m=0}^{\infty} a_m^{(1)} \cos \omega_m \, \alpha_j(t) + \sum_{m=1}^{\infty} a_m^{(2)} \sin \omega_m \, \alpha_j(t) \right) \sin \omega_m \, \alpha_j(t) dt \end{cases} \tag{6c}$$

and ω_m are the amplitudes and frequencies of the cutting fluid delivered into the milling operation. Using the fact that

$$x(t) - x\left(t - \left(\tau_2 + \varepsilon\gamma_l\left(\alpha_j(t)\right)\right)\right) := x(t) - x(t - \tau_2) + \varepsilon \int_{t-\left(\tau_2+\varepsilon\gamma_l\left(\alpha_j(t)\right)\right)}^{t-\tau_2} \dot{x}\left(t + \alpha_j(t)\right) d\alpha_j(t) \tag{6d}$$

we can write Equation (6a) as follows

$$\Delta g_{cx}\left(\alpha_j(t), \dot{m}\left(\alpha_j(t), \dot{\vartheta}_l(t)\right), \mu_2\right) \tag{6e}$$

$$= -\widetilde{w}\left\{\tilde{k}_1\left\{x(t) - x(t-\tau_1) + \varepsilon\int_{t-(\tau_1+\varepsilon\gamma_l(\alpha_j(t)))}^{t-\tau_1} \dot{x}\big(t+\alpha_j(t)\big)d\alpha_j(t)\right\}\right.$$

$$+ \tilde{k}_2\left\{x(t) - x(t-\tau_1) + \varepsilon\int_{t-(\tau_1+\varepsilon\gamma_l(\alpha_j(t)))}^{t-\tau_1} \dot{x}\big(t+\alpha_j(t)\big)d\alpha_j(t)\right\}^2$$

$$+ \tilde{k}_3\left\{x(t) - x(t-\tau_1) + \varepsilon\int_{t-(\tau_1+\varepsilon\gamma_l(\alpha_j(t)))}^{t-\tau_1} \dot{x}\big(t+\alpha_j(t)\big)d\alpha_j(t)\right\}^3$$

$$+ \cdots O\left\{\tilde{k}_5\left\{x(t) - x(t-\tau_1)\right.\right.$$

$$\left.\left.\left. + \varepsilon\int_{t-(\tau_1+\varepsilon\gamma_l(\alpha_j(t)))}^{t-\tau_1} \dot{x}\big(t+\alpha_j(t)\big)d\alpha_j(t)\right\}^5\right\}\right\}$$

The time delay τ_2 corresponds to the nominal value of the mass of the fluid delivered into the milling operation for $h_{j\kappa}\left(s_{j\kappa}, \alpha_j(t)\right)_{min} \leq h_{j\kappa}\left(s_{j\kappa}, \alpha_j(t)\right) \leq h_{j\kappa}\left(s_{j\kappa}, \alpha_j(t)\right)_{max}$ and in the interval $\alpha_{j,ent}(t) \leq \alpha_j(t) \leq \alpha_{j,exit}(t)$. This time delay τ_2 is determined by the length of travel of the coolant and velocity it travels with as it enters $\alpha_{j,ent}(t) \leq \alpha_j(t) \leq \alpha_{j,exit}(t)$. w is the width in which the coolant is delivered inside the interval $\alpha_{j,ent}(t) \leq \alpha_j(t) \leq \alpha_{j,exit}(t)$. The parameters $\tilde{k}_1, \tilde{k}_2, \cdots \tilde{k}_j, j = 1,2,3, \cdots$ represent the coefficients of the nonlinearity after Taylor expansion of $\Delta g_{cx}\left(\alpha_j(t), \dot{m}\left(\alpha_j(t), \dot{\vartheta}_l(t)\right), \mu_2\right)$ at some nominal value of the mass flow rate of the cutting fluid in the interval $\alpha_{j,ent}(t) \leq \alpha_j(t) \leq \alpha_{j,exit}(t)$. The time-varying delay parameter $\gamma_l\left(\alpha_j(t)\right)$ and the nonlinearity will continue to fluctuate no matter how small or large the induced cutting force variation $\Delta f_x\left(\alpha_j(t), \Delta h_{j\kappa}\left(s_{j\kappa}, \alpha_j(t)\right), \mu_1\right)$ is. The appearance of $\alpha_j(t)$ in the Fourier representation of the mass variation $\Delta g_{cx}\left(\alpha_j(t), \dot{m}\left(\alpha_j(t), \dot{\vartheta}_l(t)\right), \mu_2\right)$ serves to explain the correlation between this variation and that of the cutting force $\Delta f_x\left(\alpha_j(t), \Delta h_{j\kappa}\left(s_{j\kappa}, \alpha_j(t)\right), \mu_1\right)$ in the interval $\alpha_{j,ent}(t) \leq \alpha_j(t) \leq \alpha_{j,exit}(t)$. The angular position of the nozzles, which is freely adjusted to different positions between the machine-tool spindle and work piece and oil or chip contaminants, may transport high gravitational and damping torques as the cutting fluid enters in the interval $\alpha_{j,ent}(t) \leq \alpha_j(t) \leq \alpha_{j,exit}(t)$. The Fourier representation of $\Delta g_{cx}\left(\alpha_j(t), \dot{m}\left(\alpha_j(t), \dot{\vartheta}_l(t)\right), \mu_2\right)$ in Equation (6) thus gives us better estimates of the amplitudes and frequencies of the cutting fluid delivered into j-teeth of the milling cutter at $\alpha_{j,ent}(t) \leq \alpha_j(t) \leq \alpha_{j,exit}(t)$ and of depth of cut d and chip thickness $h_{j\kappa}\left(s_{j\kappa}, \alpha_j(t)\right)_{min} \leq h_{j\kappa}\left(s_{j\kappa}, \alpha_j(t)\right) \leq h_{j\kappa}\left(s_{j\kappa}, \alpha_j(t)\right)_{max}$. The Fourier representation has a sufficient structure to evaluate relationships and phenomena for long term variations of both $\Delta f_x\left(\alpha_j(t), \Delta h_{j\kappa}\left(s_{j\kappa}, \alpha_j(t)\right), \mu_1\right)$ and $\Delta g_{cx}\left(\alpha_j(t), \dot{m}\left(\alpha_j(t), \dot{\vartheta}_l(t)\right), \mu_2\right)$. The amplitudes, frequencies and stability regimes of the milling operation of various mass of the cutting fluid in the interval $\alpha_{j,ent}(t) \leq \alpha_j(t) \leq \alpha_{j,exit}(t)$ can be calculated in a more direct way. The threshold of the attainable variations of $\Delta f_x\left(\alpha_j(t), \Delta h_{j\kappa}\left(s_{j\kappa}, \alpha_j(t)\right), \mu_1\right)$ and $\Delta g_{cx}\left(\alpha_j(t), \dot{m}\left(\alpha_j(t), \dot{\vartheta}_l(t)\right), \mu_2\right)$ is represented by the finite nature of the nonlinearities and sizes of the time varying delays. Generalization of this representation to other forms of cutting fluids and machining operations is attainable as well. The small parameter ε has values of the form $0 \leq \varepsilon \ll 1$, and it is scaling factor of the nonlinearities in $\Delta f_x\left(\alpha_j(t), \Delta h_{j\kappa}\left(s_{j\kappa}, \alpha_j(t)\right), \mu_1\right)$ and $\Delta g_{cx}\left(\alpha_j(t), \dot{m}\left(\alpha_j(t), \dot{\vartheta}_l(t)\right), \mu_2\right)$. The next section is concerned with the aspects of deriving the cutting force variation $\Delta f_x\left(\alpha_j(t), \Delta h_{j\kappa}\left(s_{j\kappa}, \alpha_j(t)\right), \mu_1\right)$ in terms of the chip thickness variation $\Delta h_{j\kappa}\left(s_{j\kappa}, \alpha_j(t)\right)$.

5.3. The Cutting Fluid Force in Machining

The cutting force variation along the x-direction as seen in Figure 8 is given by

$$\Delta f_x\left(\alpha_j(t), \Delta h_{j\kappa}\left(s_{j\kappa}, \alpha_j(t)\right), \mu_1\right) = -w\sum_{j=1}^{z_j} \chi_{j\kappa}\left(\alpha_j(t), z_{jc}\right) \times f_{jx}\left(\Delta h_{j\kappa}\left(s_{j\kappa}, \alpha_j(t), d\right) k_{jx}\left(\alpha_j(t), \mu_1\right)\right) \tag{7}$$

where $f_{jx}\left(\Delta h_{j\kappa}\left(s_{j\kappa}, \alpha_j(t), d\right)\right)$ is the cutting force variation that is dependent only on the feed $\Delta h_{j\kappa}\left(s_{j\kappa}, \alpha_j(t)\right)$ per tooth and depth of cut d. $k_{jx}\left(\alpha_j(t), \mu_1\right)$ is the cutting force coefficient per unit area and is equivalent to $F_{jx}\left(\alpha_j(t), \mu_1\right)$. By the geometry of the cutter-workpiece interaction in Figure 15 we have the expressions for $\Delta h_{j\kappa}\left(s_{j\kappa}, \alpha_j(t)\right)$ and $F_{jx}\left(\alpha_j(t), \mu_1\right)$, as follows

$$h_{j\kappa}\left(s_{j\kappa}, \alpha_j(t)\right) = s_{j\kappa} \sin \alpha_j(t) \tag{8a}$$

with

$$\Delta h_{j\kappa}\left(s_{j\kappa}, \alpha_j(t)\right) = h_{j\kappa}\left(s_{j\kappa}, \alpha_j(t)\right)_{chatter} - h_{j\kappa}\left(s_{j\kappa}, \alpha_j(t)\right)_{zeroc\,hatter} \tag{8b}$$

$$= \left(s_{j0} + x(t) - x\left(t - \tau_j(t)\right)\right)\sin\alpha_j(t) - s_{j0}\sin\alpha_j(t)$$

$$= \left(x(t) - x\left(t - \tau_j(t)\right)\right)\sin\alpha_j(t)$$

and the cutting force

$$F_{jx}\left(\alpha_j(t), \mu_1\right) = F_{jt}\,\cos\alpha_j(t) + F_{jr}\,\sin\alpha_j(t) \tag{8c}$$

with the relationship $F_{jr} = F_{jt}\,\tan\beta$ yield

$$F_{jx}\left(\alpha_j(t), \mu_1\right) = F_{jt}\,\cos\alpha_j(t) + F_{jt}\,\tan\beta\sin\alpha_j(t) = F_{jt}\left\{\cos\alpha_j(t) + \tan\beta\sin\alpha_j(t)\right\} \tag{8d}$$

$$= \sqrt{1+\tan^2\beta}\,F_{jt}\,\cos\left(\alpha_j(t) - \vartheta_0\right)$$

where

$$\cos\vartheta_0 = \frac{1}{\sqrt{1+\tan^2\beta}}, \quad \sin\vartheta_0 = \frac{\tan\beta}{\sqrt{1+\tan^2\beta}} \tag{8e}$$

and this lead to the simplification of Equation (7) into the form

$$\Delta f_x\left(\alpha_j(t), \Delta h_{j\kappa}\left(s_{j\kappa}, \alpha_j(t)\right), \mu_1\right) \tag{8f}$$

$$= -\sqrt{1+\tan^2\beta}\, w \sum_{j=1}^{z_j} \chi_{j\kappa}\left(\alpha_j(t), z_{jc}\right)$$

$$\times f_{jx}\left(\Delta h_{j\kappa}\left(s_{j\kappa}, \alpha_j(t), d\right) k_{jx}\left(\alpha_j(t), \mu_1\right) \cos\left(\alpha_j(t) - \vartheta_0\right) \sin \alpha_j(t)\right)$$

The minus sign $-\Delta f_x$ of the cutting force variation of the j-tooth indicates that a positive relative displacement of the cutter removes a feed $h_{j\kappa}\left(s_{j\kappa}, \alpha_j(t)\right)$ per tooth of material and at depth of cut d. s_{j0} is the segment at the steady state nominal feed per j-tooth of the milling cutter. $x(t)$ is the state of the milling cutter and $x(t-\tau(t))$ is the earlier state $x(t-\tau(t))$ at time $t-\tau_j(t)$. It is known that cutting force $F_{jt} = F_{jt}\left(w, r, d, h_{j\kappa}\left(s_{j\kappa}, \alpha_j(t)\right)\right)$ is function of the cutting parameters, namely, the width of cut w, feedrate r, depth of cut d and feed per tooth $h_{j\kappa}\left(s_{j\kappa}, \alpha_j(t)\right)$. For the depth of cut variation, we define the corresponding cutting force coefficients $k_{jx}\left(\alpha_j(t), \mu_1\right)$ as follow

$$k_{jx}\left(\alpha_j(t), \mu_1\right) := -\left\{\frac{\partial^j F_{jt}\left(w, r, d, h_{j\kappa}\left(s_{j\kappa}, \alpha_j(t)\right)\right)}{j!\,\partial d^j}\right\}_{d=d_0} \tag{9}$$

$$= k_1 + k_2(k_1), k_3(k_1), + \cdots k_{j+1}(k_1), \quad j = 1,2,3, \cdots$$

where $\frac{\partial^j F_{jt}(\cdot)}{j!\partial d^j}$ are j-partial derivatives of $F_{jt}\left(w, r, d, h_{j\kappa}\left(s_{j\kappa}, \alpha_j(t)\right)\right)$ with respect to d. And k_j are the respective cutting coefficients after the Taylor expansion of $F_{jt} = F_{jt}\left(w, r, d, h_{j\kappa}\left(s_{j\kappa}, \alpha_j(t)\right)\right)$. Next we consider the Taylor expansion of

$f_{jx}\left(\Delta h_{j\kappa}\left(s_{j\kappa}, \alpha_j(t)\right), d\right)$ with respect to the feed $h_{j\kappa}\left(s_{j\kappa}, \alpha_j(t)\right)$ per tooth and compute the Taylor coefficients at depth of cut $d = d_0$, thus we obtain

$$f_{jx}\left(\Delta h_{j\kappa}\left(s_{j\kappa}, \alpha_j(t)\right), d\right) \tag{10a}$$
$$= (1!)^{-1} f_{jx}^{(1)}(d_0)\big(x(t) - x(t - \tau_j(t))\big) \sin \alpha_j(t)$$
$$+ (2!)^{-1} f_{jx}^{(2)}(d_0)\big\{\big(x(t) - x(t - \tau_j(t))\big) \sin \alpha_j(t)\big\}^2$$
$$+ (3!)^{-1} f_{jx}^{(3)}(d_0)\big\{\big(x(t) - x(t - \tau_j(t))\big) \sin \alpha_j(t)\big\}^3$$
$$+ \cdots O\left\{f_{jx}^{(5)}(d_0)\big\{\big(x(t) - x(t - \tau_j(t))\big) \sin \alpha_j(t)\big\}^5\right\}$$

where $f_{jx}\left(\Delta h_{j\kappa}\left(s_{j\kappa}, \alpha_j(t)\right), d\right), j = 1,2, \cdots$ are again the partial derivatives and comparing this Equation (10a) with Equation (9), we have

$$f_{jx}\left(\Delta h_{j\kappa}\left(s_{j\kappa}, \alpha_j(t)\right), d\right) \tag{10b}$$
$$= k_1\big(x(t) - x(t - \tau_j(t))\big) \sin \alpha_j(t)$$
$$+ k_2\big\{\big(x(t) - x(t - \tau_j(t))\big) \sin \alpha_j(t)\big\}^2$$
$$+ k_3\big\{\big(x(t) - x(t - \tau_j(t))\big) \sin \alpha_j(t)\big\}^3$$
$$+ \cdots O\left\{k_5\big\{\big(x(t) - x(t - \tau_j(t))\big) \sin \alpha_j(t)\big\}^5\right\}$$

Hence the substitution of Equations (9) and (10) into (8) gives

$$\Delta f_x\left(\alpha_j(t), \Delta h_{j\kappa}\left(s_{j\kappa}, \alpha_j(t)\right), \mu_1\right) \tag{11}$$

$$= -w\sum_{j=1}^{z_j} \chi_{j\kappa}\left(\alpha_j(t), z_{jc}\right)\cos\left(\alpha_j(t)-\vartheta_0\right)\Big\{k_1\big(x(t)-x(t$$

$$-\tau_j(t))\sin\alpha_j(t) + k_2\left\{\left(x(t)-x(t-\tau_j(t)\right)\sin\alpha_j(t)\right\}^2$$

$$+ k_3\left\{\left(x(t)-x(t-\tau_j(t)\right)\sin\alpha_j(t)\right\}^3$$

$$+ \cdots O\left\{k_5\left\{\left(x(t)-x(t-\tau_j(t)\right)\sin\alpha_j(t)\right\}^5\right\}\Big\}$$

Now using the fact that $\tau_j(t) = \tau_2 + \varepsilon\gamma_j(\alpha_j(t))$ so that

$$x(t) - x\left(t - \left(\tau_2 + \varepsilon\gamma_j(\alpha_j(t))\right)\right) := x(t) - x(t-\tau_2) \tag{12a}$$

$$+ \varepsilon\int_{t-\left(\tau_2+\varepsilon\gamma_j(\alpha_j(t))\right)}^{t-\tau_2} \dot{x}\left(t+\alpha_j(t)\right)d\alpha_j(t)$$

We thus obtain the period cutting function $\Delta f_x\left(\alpha_j(t), \Delta h_{j\kappa}\left(s_{j\kappa}, \alpha_j(t)\right), \mu_1\right)$ as follows

$$\Delta f_x\left(\alpha_j(t), \Delta h_{j\kappa}\left(s_{j\kappa}, \alpha_j(t)\right), \mu_1\right) \tag{12b}$$

$$= -w\left\{k_1\left\{x(t) - x(t-\tau_2) + \varepsilon\int_{t-\left(\tau_2+\varepsilon\gamma_j(\alpha_j(t))\right)}^{t-\tau_2} \dot{x}\big(t+\alpha_j(t)\big)d\alpha_j(t)\right\}\right.$$

$$+ k_2\left\{x(t) - x(t-\tau_2) + \varepsilon\int_{t-\left(\tau_2+\varepsilon\gamma_j(\alpha_j(t))\right)}^{t-\tau_2} \dot{x}\big(t+\alpha_j(t)\big)d\alpha_j(t)\right\}^2$$

$$+ k_3\left\{x(t) - x(t-\tau_2) + \varepsilon\int_{t-\left(\tau_2+\varepsilon\gamma_j(\alpha_j(t))\right)}^{t-\tau_2} \dot{x}\big(t+\alpha_j(t)\big)d\alpha_j(t)\right\}^3$$

$$+ \cdots O\left\{k_5\left\{x(t) - x(t-\tau_2)\right.\right.$$

$$\left.\left.\left. + \varepsilon\int_{t-\left(\tau_2+\varepsilon\gamma_j(\alpha_j(t))\right)}^{t-\tau_2} \dot{x}\big(t+\alpha_j(t)\big)d\alpha_j(t)\right\}^5\right\}\right\}$$

where the time-varying regenerative delay $\tau_l\big(\alpha_j(t), z_{jc}, \Omega\big)$ is defined by

$$\begin{cases} \tau_j\big(\alpha_j(t), z_{jc}, \Omega\big) = \tau_2 + \varepsilon\gamma\left(\alpha_j(t)\right), \qquad 0 \le \varepsilon \ll 1 \\ \gamma\left(\alpha_j(t)\right) = \sum_{m=0}^{\infty} b_m^{(1)}\cos\omega_m\,\alpha_j(t) + \sum_{m=1}^{\infty} b_m^{(2)}\sin\omega_m\,\alpha_j(t) \end{cases} \tag{12c}$$

and the Fourier constants $b_m^{(0)}$, $b_m^{(1)}$and $b_m^{(2)}$, namely

$$\begin{cases} b_m^{(0)} = \dfrac{1}{\Gamma(\alpha_j(t), z_{jc}, \Omega)} \cdot \\ \displaystyle\int_0^{\Gamma(\alpha_j(t), z_{jc}, \Omega)} \left(\sum_{m=0}^{\infty} b_m^{(1)} \cos \widetilde{\omega}_m \, \alpha_j(t) + \sum_{m=1}^{\infty} b_m^{(2)} \sin \widetilde{\omega}_m \, \alpha_j(t) \right) d\alpha_j(t) \\ b_m^{(1)} = \dfrac{1}{\Gamma(\alpha_j(t), z_{jc}, \Omega)} \cdot \\ \displaystyle\int_0^{\Gamma(\alpha_j(t), z_{jc}, \Omega)} \left(\sum_{m=0}^{\infty} b_m^{(1)} \cos \widetilde{\omega}_m \, \alpha_j(t) + \sum_{m=1}^{\infty} b_m^{(2)} \sin \widetilde{\omega}_m \, \alpha_j(t) \right) \cos \widetilde{\omega}_m \, \alpha_j(t) dt \\ b_m^{(2)} = \dfrac{1}{\Gamma(\alpha_j(t), z_{jc}, \Omega)} \cdot \\ \displaystyle\int_0^{\Gamma(\alpha_j(t), z_{jc}, \Omega)} \left(\sum_{m=0}^{\infty} b_m^{(1)} \cos \widetilde{\omega}_m \, \alpha_j(t) + \sum_{m=1}^{\infty} b_m^{(2)} \sin \widetilde{\omega}_m \, \alpha_j(t) \right) \sin \widetilde{\omega}_m \, \alpha_j(t) dt \end{cases} \tag{12d}$$

Substituting Equations (6) and (12) into (1), and using only the linear part of Equations (6) we obtain the following equation

$$\begin{aligned} &\ddot{x} + 2\zeta\omega_0\dot{x} + {\omega_0}^2\mu_1\big(x - x(t-\tau_1)\big) + {\omega_0}^2\mu_2\big(x - x(t-\tau_2)\big) \\ &\qquad = -\varepsilon{\omega_0}^2\sigma_3\left\{x - x(t-\tau_2) + \int_{t-\tau(t)}^{t-\tau_2} \dot{x}(t+\theta)d\theta\right\}^3 - O(\varepsilon^5) \end{aligned} \tag{13}$$

where $\varepsilon\sigma_3$ denotes the presence of the nonlinearity of the cutting force variation

We study the linear stability of this equation so as to establish regimes of stable milling process and safe coolant penetration forces.

5.4. Linear Stability Analysis

The linear stability of Equation (12) is examined by considering the linearized solutions to the delay differential equation

$$\ddot{x} + 2\zeta\omega_0\dot{x} + \omega_0^2 x + \omega_0^2\mu_1\big(x - x(t-\tau_1)\big) + \omega_0^2\mu_2\big(x - x(t-\tau_2)\big) = 0 \tag{13a}$$

whose transcendental characteristic equation is

$$\Delta(\lambda, \mu^1, \mu^2) := \lambda^2 + 2\zeta\omega_0\lambda + \omega_0^2 + \omega_0^2\{\mu_1(1 - e^{-\lambda\tau_1}) + \mu_2\,(1 - e^{-\lambda\tau_2})\} = 0 \tag{13b}$$

is obtained after making the substitutions $x(t) = exp(\lambda t)$, $x(t-\tau) = exp(\lambda(t-\tau))$ and $\tau \in [\tau_1, \tau_2]$. The force coefficient μ_1 is considered as the bifurcation that is continuously perturbed by a small value $\varepsilon\mu_1$ at its critical value μ_{1c} and we write $\mu_1 = \mu_{1c} + \varepsilon\mu$. By Hopf bifurcation conditions [21-22] and reference cited therein, we let $\lambda_{1,2} = v(\mu_1) \pm j\omega(\mu_1)$, $j = \sqrt{-1}$ with $v(\mu_1) > 0$, $\omega(\mu_1) \neq 0$ and $v(\mu_{1c}) = 0$, $\Re e\{d\Delta(\lambda, \mu_1, \mu_2)/d\mu_1\} \neq 0$ be the eigenvalues of (4b). All the remaining eigenvalues of $\Delta(\lambda, \mu_1, \mu_2) = 0$ have negative real parts. Then, the substitution of $\lambda_1 = v(\mu_1) + j\omega(\mu_1)$ into $\Delta(\lambda, \mu_1, \mu_2) = 0$, and setting the real and imaginary parts of the resulting algebraic equations to zero, we have

$$\Delta(\lambda, \mu^1, \mu^2) := G^{111}(\lambda, \mu^1, \mu^2) + jM^{111}(\lambda, \mu^1, \mu^2) = 0, \quad j = \sqrt{-1} \tag{14a}$$

where the symbols $G_{111}(\lambda, \mu_1, \mu_2)$ and $M_{111}(\lambda, \mu_1, \mu_2)$ denote the real and imaginary parts accordingly

$$\begin{cases} G_{111}(\lambda, \mu_1, \mu_2) := v^2 + \omega_0^2 - \omega^2 + 2\zeta\omega_0 v + \omega_0^2 \begin{Bmatrix} \mu_1(1 - e^{-\lambda\tau_1}\cos\omega\tau_1) + \\ \mu_2\,(1 - e^{-\lambda\tau_2}\cos\omega\tau_2) \end{Bmatrix} = 0 \\ M^{111}(\lambda, \mu^1, \mu^2) := 2(v + \zeta\omega_0)\omega - \omega_0^2\,\{\mu_1 e^{-\lambda\tau_1}\sin\omega\tau_1 + \mu_2 e^{-\lambda\tau_2}\sin\omega\tau_2\} = 0 \end{cases} \tag{14b}$$

and by putting $\upsilon = 0$ at Hopf bifurcation yields

$$\begin{cases} G_{111}(\lambda, \mu_1, \mu_2) := \omega_0^2 - \omega^2 + \omega_0^2\{\mu_1(1-\cos\omega\tau_1) + \mu_2\,(1-\cos\omega\tau_2)\} = 0 \\ M^{111}(\lambda, \mu) := 2\zeta\omega_0\omega - \omega_0^2\{\mu_1 \sin\omega\tau_1 + \mu_2 \sin\omega\tau_2\} = 0 \end{cases} \tag{14c}$$

or equivalently

$$\begin{cases} \omega_0^2\mu_1(1-\cos\omega\tau_1) = -\{(\omega_0^2 - \omega^2) + \omega_0^2\,\mu_2\,(1-\cos\omega\tau_2)\} \\ \omega_0^2\mu_1 \sin\omega\tau_2 = 2\zeta\omega_0\omega - \omega_0^2\mu_2 \sin\omega\tau_2 \end{cases} \tag{14d}$$

Now squaring both sides of Equations (14d) and adding the result together will lead to

$$2\omega_0^4\mu_1^2(1-\cos\omega\tau_1) \tag{15a}$$
$$= \{(\omega_0^2 - \omega^2) + \omega_0^2\,\mu_2\,(1-\cos\omega\tau_2)\}^2 + \{2\zeta\omega_0\omega - \omega_0^2\mu_2\sin\omega\tau_2\}^2$$

where the substitution of the first equation in (14d) into (15a), namely

$$2\omega_0^2\mu_1\{(\omega_0^2 - \omega^2) + \omega_0^2\,\mu_2\,(1-\cos\omega\tau_2)\} \tag{15b}$$
$$= \{(\omega_0^2 - \omega^2) + \omega_0^2\,\mu_2\,(1-\cos\omega\tau_2)\}^2 + \{2\zeta\omega_0\omega - \omega_0^2\mu_2\sin\omega\tau_2\}^2$$

and thus we obtain the explicit expression for the bifurcation parameter μ_1

$$\mu_1(\tau_1, \tau_2, \omega, \mu_2) = \frac{1}{2\omega_0^2 r_{112}}(r_{111}^2 + r_{112}^2) \tag{15c}$$

with r_{111} and r_{112} donating

$$\begin{cases} r_{111} = -\{(\omega_0^2 - \omega^2) + \omega_0^2 \mu_2 (1 - \cos \omega\tau_2)\} \\ r_{112} = 2\zeta\omega_0\omega - \omega_0^2\mu_2 \sin \omega\tau_2 \end{cases} \tag{15d}$$

We compute Hopf's transversality condition by differentiating implicitly (13b) with respect to μ_1, namely

$$\frac{d}{d\mu_1}\{\Delta(\lambda, \mu_1, \mu_2)\} = \frac{d\Delta(\lambda, \mu_1, \mu_2)}{d\lambda} \times \frac{d\lambda}{d\mu_1} + \frac{d\Delta(\lambda, \mu_1, \mu_2)}{d\mu_1} = 0 \tag{16a}$$

from which the real and imaginary parts when $\lambda_{1,2} = \upsilon(\mu_1) \pm j\omega(\mu_1)$ are given by

$$\begin{aligned} \left(\frac{d\lambda}{d\mu_1}\right)_{\lambda_{1,2}=\upsilon(\mu_1)\pm j\omega(\mu_1)} &= -\left(\frac{d\Delta(\lambda, \mu_1, \mu_2)}{d\mu_1}\right)\left(\frac{d\Delta(\lambda, \mu_1, \mu_2)}{d\lambda}\right)^{-1}\Bigg\}_{\lambda_{1,2}=\upsilon(\mu_1)\pm j\omega(\mu_1)} \\ &= -\frac{\omega_0^2 (1 - \cos \omega\tau_1 + j \sin \omega\tau_1)}{r_{113} + jr_{114}}\Bigg\}_{\lambda_{1,2}=\upsilon(\mu_1)\pm j\omega(\mu_1), \upsilon(\mu_{1c})=0} \\ &:= G_{222}(\lambda, \mu_1, \mu_2) + jM_{222}(\lambda, \mu_1, \mu_2)\}_{\lambda_{1,2}=\upsilon(\mu_1)\pm j\omega(\mu_1), \upsilon(\mu_{1c})=0} \end{aligned} \tag{16b}$$

where by writing

$$\left(\frac{d\lambda}{d\mu_1}\right)_{\lambda_{1,2}=\upsilon(\mu_1)\pm j\omega\,(\mu_1)} \tag{16c}$$

$$= -\frac{\omega_0^2\,(1-\cos\omega\tau_1 + j\sin\omega\tau_1)}{r_{113}+jr_{114}}\Bigg\}_{\lambda_{1,2}=\upsilon(\mu_1)\pm j\omega\,(\mu_1),\upsilon(\mu_{1c})=0}$$

$$:= G_{222}(\lambda,\mu_1,\mu_2) + jM_{222}(\lambda,\mu_1,\mu_2)\}_{\lambda_{1,2}=\upsilon(\mu_1)\pm j\omega\,(\mu_1),\upsilon(\mu_{1c})=0}$$

with the notations r_{113}, r_{114}, $G_{222}(\lambda,\mu_1,\mu_2)$, $M_{222}(\lambda,\mu_1,\mu_2)$:

$$\begin{cases} G_{222}(\lambda,\mu_1,\mu_2) = -\dfrac{1}{r_{113}^2+r_{114}^2}\left\{\omega_0^2\big((1-\cos\omega\tau_1)r_{113}+\sin\omega\tau_1\, r_{114}\big)\right\} \\ M_{222}(\lambda,\mu_1,\mu_2) = -\dfrac{1}{r_{113}^2+r_{114}^2}\left\{\omega_0^2\big((1-\cos\omega\tau_1)r_{114}-\sin\omega\tau_1\, r_{113}\big)\right\} \end{cases} \tag{16d}$$

$$\begin{cases} r_{113} = 2\zeta\omega_0 + \omega_0^2\tau_1\mu_1\cos\omega\tau_1 + \omega_0^2\tau_2\mu_2\cos\omega\tau_2 \\ r_{114} = 2\omega - \omega_0^2\tau_1\mu_1\sin\omega\tau_1 + \omega_0^2\tau_2\mu_2\sin\omega\tau_2 \end{cases} \tag{16e}$$

and thus it can be seen that

$$\Re\left(\frac{d\lambda}{d\mu_1}\right)_{\lambda_{1,2}=\upsilon(\mu_1)\pm j\omega\,(\mu_1),\upsilon(\mu_{1c})=0} = G_{222}(\lambda,\mu_1,\mu_2)_{\lambda_{1,2}=\upsilon(\mu_1)\pm j\omega\,(\mu_1),\upsilon(\mu_{1c})=0} > 0 \tag{16f}$$

if the choice of values for the model parameters are such that the inequality (16g) holds.

$$\omega_0^2\big((1-\cos\omega\tau_1)r_{113}+\sin\omega\tau_1\, r_{114}\big) < 0 \tag{16g}$$

This means that the pair of eigenvalues $\lambda_{1,\,2} = \upsilon(\mu_1) \pm j\omega(\mu_1)$ of $\Delta(\lambda,\mu_1,\mu_2) = 0$ with $\upsilon(\mu_{1c}) = 0$, $\omega(\mu_{1c}) \neq 0$ will cross the imaginary axis from left to right in the complex plane with a nonzero speed as the bifurcation parameter μ_1 varies near its critical value μ_{1c}. Also, it ensures that the steady state stability of the system is lost at $\mu_1 = \mu_{1c}$.

We derive the explicit expression for τ_2 by rewriting equations (5d) as follows

$$\frac{\omega_0^2(1-\cos\omega\tau_1)}{\omega_0^2\mu_1\sin\omega\tau_1} = -\frac{\omega_0^2-\omega^2+\omega_0^2\mu_2(1-\cos\omega\tau_2)}{2\zeta\omega_0\omega-\omega_0^2\mu_2\sin\omega\tau_2} = \frac{r_{111}}{r_{112}} \tag{17a}$$

or equivalently

$$\frac{1-\cos\omega\tau_1}{\sin\omega\tau_1} = \frac{r_{111}}{r_{112}} \tag{17b}$$

where using the fact that $\cos^2\omega\tau_1 + \sin^2\omega\tau_1 = 1$ and the trigonometric identity

$$tan(\frac{\omega\tau_1}{2}) = \sqrt{\frac{\sin^2\frac{\omega\tau_1}{2}}{\cos^2\frac{\omega\tau_1}{2}}} = \sqrt{\frac{1/2(1-cos\omega\tau_1)}{1/2(1+cos\omega\tau_1)}} = \sqrt{\frac{(1-cos\omega\tau_1)(1-cos\omega\tau_1)}{(1+cos\omega\tau_1)(1-cos\omega\tau_1)}} \tag{17c}$$

$$= \sqrt{\frac{(1-cos\omega\tau_1)^2}{(sin^2\omega\tau_1)}} = \left|\frac{(1-cos\omega\tau_1)}{sin\omega\tau_1}\right| = \frac{1-cos\omega\tau_1}{sin\omega\tau_1}$$

so that

$$\left(\frac{\omega\tau_1}{2}\right) = arctan\left(\frac{r_{111}}{r_{112}}\right) + \pi\kappa, \kappa = ,1,2,3,\cdots n,\cdots \tag{17d}$$

and thus we obtain

$$\tau_1 = \frac{2}{\omega}\{arctan(\frac{r_{111}}{r_{112}}) + \pi\kappa\}, \kappa = ,1,2,3, \cdots n, \cdots \tag{17e}$$

and with $\tau_1 = 2\pi/(z_c\Omega)$, we get the spindle expression

$$\Omega = \frac{2\pi}{z_c\tau_1} = \frac{\pi\omega}{\tan^{-1}\left(\frac{r_{111}}{r_{112}}\right)}, \kappa = ,1,2,3, \cdots n, \cdots \tag{17f}$$

Using Equations (15) and (17), we obtain the stability charts as presented in Figure 25 and Figure 26 for the following cases: 1) cutting without cutting fluids, 2) cutting with cutting fluids. All the stability charts are plotted using Matlab and the constants selected are listed below [33].

Natural Frequency	$\omega_0 = 6038.7\ Hz$
Damping Factor	$\zeta = 0.025\%$
Nominal Time Delay for Cutting Fluid Factor	$\tau_2 = 3.5 \times 10^{-4}$

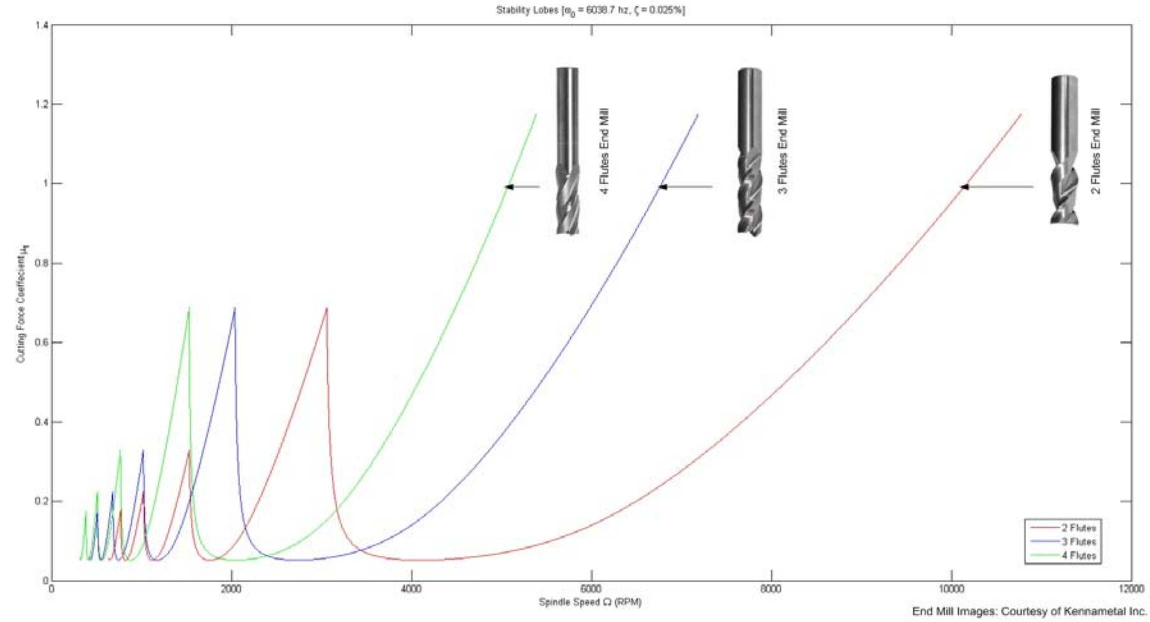

Figure 25: Stability lobes - Cutting without cutting fluid [2 flutes, 3 flutes and 4 flutes]

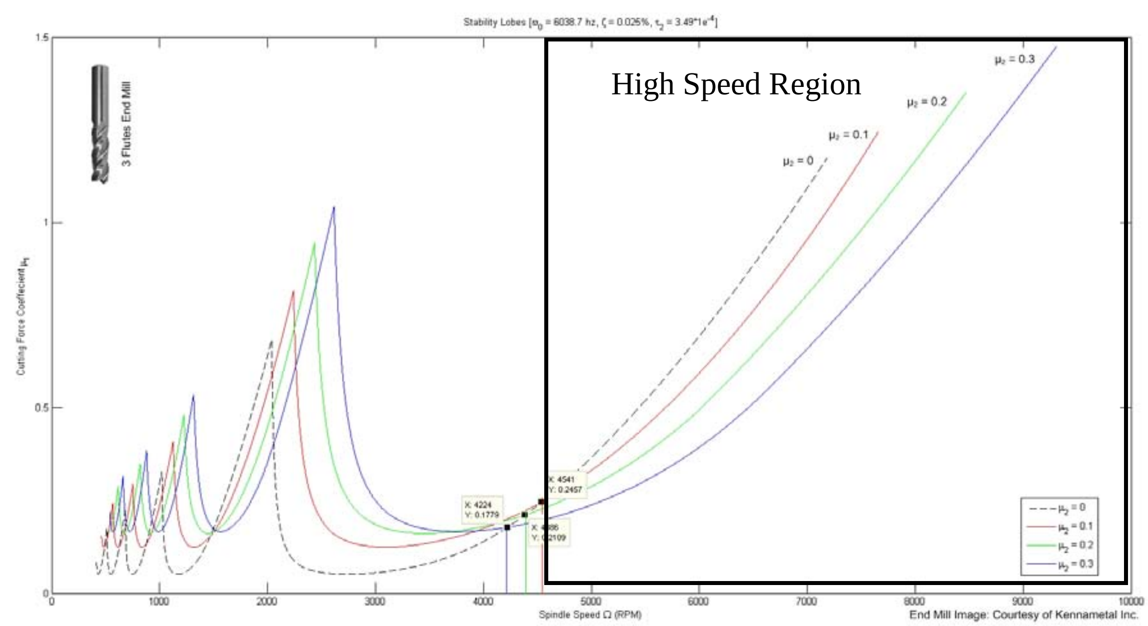

Figure 26: Stability lobes - Cutting with varying penetration force of cutting fluid

Chapter 6. Results and Discussions

Based on the study and the stability charts we obtain, a correlation between process regenerative chatter and the penetration force of cutting fluid is observed and quantified as follows:

1) The study shows that the end mill with more flutes delivers better stability regimes. However for machining soft material like aluminum, fewer flutes are preferred to remove chips continuously. The result points to the selection of three flutes for widening the stability regimes.

2) In high speed machining (Spindle speed > 6000RPM), when we assumed that all the other machining constants and variables are not changed and the penetration force of cutting fluid is more significant than other disturbance factors, increased penetration force of the cutting fluid will reduce the stability region of the machining proportionally.

3) From the stability chart, we observe that dry machining at high spindle speed is preferred within our model. However, the use of cutting fluid is necessary in order to control the machining temperature and remove chips continuously. Generally, these disturbance factors such as the temperature, lubrication and chips were not considered in this research.

4) The accurate selection of the penetration force of the cutting fluid is of great importance if one is to balance among the concerns of regenerative chatter, cutting fluid contaminants, penetration forces and high temperatures.

Several preceding studies were also reviewed to compare with our results obtained here. Ezugwu et al. [42] have tried to machine nickel-base Inconel 718 alloy with ceramic tools under finishing conditions with various coolant supply pressures. In their experiment, they cut the same material with three sets of cutting speed: 200 m/min, 270 m/min and 300 m/min and two sets of feed rate: 0.1 mm/rev and 0.2 mm/rev while the depth of cut was held always. The cutting fluid they used for trials was a high lubricity emulsion coolant containing alkanolamine salts of the fatty acid and dicyclohexylamine. The concentration of the coolant was six percent. Then they applied three different pressure of cutting fluid: 11 MPa, 15 MPa and 20.3 MPa. Cutting forces, tool life, surface roughness and surface integrity were four considerations as results of the trials. Some of the results were reported based on their experiment: Lower tool life were generated when machining with the highest pressure of the coolant jet (20.3 MPa) and accelerated notch wear on both flank and rake faces of the ceramic tool during machining were more significant when increasing the pressure of the coolant jet. Both of these results will reflect our analytical results to some extent. And lower cutting forces were generated when machining at higher coolant supply due to improved cooling and lubrication at the cutting interface and as a result of chip segmentation caused by the high pressure coolant jet. For cutting force, another similar research has done by Mazurkiewicz et al. [43]. They cut 1020 steel for all the trials with different pressure of coolant: 70 MPa, 140 MPa, 210 MPa and 280 MPa. Their results (Figure 27) showed that when increasing the pressure of the coolant jet proportionally, the cutting force was reduced mainly due to the cooling and lubrication enhancement. However it should be paid attention that the decreasing speed (slope) was significantly slowed when increasing the coolant pressure. This phenomenon was not specified and analyzed in their research. And it could be highly possible to be caused by the results from our model. Besides both Mazurkiewicz et al. and Sharma et al. [44] have mentioned respectively in their papers that the cooling and lubrication of the tool-chip interface by the coolant jets can account for the reduction in friction in the contact region between the tool and the workpiece and the generation of the short curl chip which may also affect the machining stability.

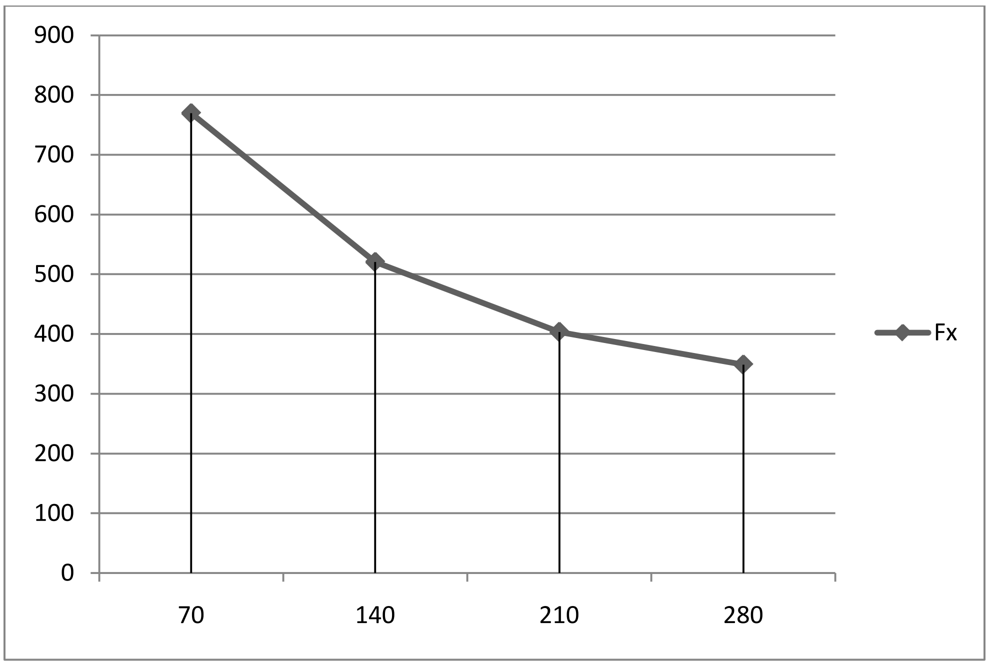

Figure 27: Cutting force under different pressure of coolant

To fully understand the impact of the penetration force of the cutting fluid and its correlation with machining stability for wide-range materials would require the analysis of nonlinear effect. The study of nonlinear effect is a recommended future work.

Chapter 7. Conclusion

Today, there are increasing efforts to discover ways to optimize machining processes. Among all the manufacturing processes, machining creates great financial wealth. With the rapid advancement of numerically controlled machine tools and the ability to design and simulate complex machining task with CAD/CAM software, high speed milling operations, for example, now provide industries an opportunity to remove substantial volumes of materials at super high feeds and spindle speeds. In this thesis, we have established a direct correlation between the penetration force of the cutting fluid and stability of the milling process at specific spindle speeds. A mathematical model is constructed and the governing equations are derived in terms of the cutting conditions, the coolant penetration force and mass flow rate. Stability charts are constructed with and without the penetration force of the coolant. It is found that by increasing the penetration force of the coolant, the machining stability regimes become narrow when other machining variables are assumed not to be changed. The study also shows how changing number of the flutes impact stable spindle speed. It is discovered that the use of higher number of flutes in process milling expands the regimes of stability.

References

1. **Aronson, R. B.** Machine Tool 101: Part 6, Machine Servers. *Manufacturing Engineering.* 6 1994, pp. 47-52.

2. **Iowa Waste Reduction Center.** *Cutting Fluid Management - Small Machining Operations.* Cedar Falls, Iowa : s.n., 2003.

3. **Koelsch, J. R.** Honing Fluid Performance. *Manufacturing Engineering.* 2 1994, pp. 51-55.

4. **Bienkowski, K.** Coolants & Lubricants - The Truth. *Manufacuturing Engineering.* 3 1993, pp. 90-96.

5. **Foltz, G.** Definitions of Metalworking Fluids. 1990.

6. **Oberg, E., et al.** *Machinery's Handbook.* New York City, NY : Industrial Press Inc., 1992. p. 2543.

7. **Stocker, W. M. and Hicks, T.** *Metalcutting: Today's Techniques for Engineers and Shop Personnel.* s.l. : McGraw-Hill, 1979. p. 182.

8. **Hope, D. A.** Cutting fluids - Pet or pest. *Tribology International.* 2 1977, pp. 23-27.

9. **Tuholski, R. J.** Don't Forget the Cutting Fluid. *Journal of Industrial Technology.* Fall 1993, pp. 2-5.

10. **Wikipedia.org.** Cutting fluid - Wikipedia, the free encyclopedia. *Wikipedia.* [Online] 2 13, 2010. [Cited: 4 11, 2010.] http://en.wikipedia.org/wiki/Cutting_fluid.

11. *The Essential for Choosing the Right Cutting Fluid.* **Valcool, V.** s.l. : Modern Application News, 9 2002.

12. **Hoobler, G. L.** *Coolant Management: A User's Introduction and Guide to Waste Minimization.*

13. **Cassin, C. and Boothroyd, G.** Lubrication action of cutting fluids. *Journal of Mechanical Engineering Science.* 3 1965, Vol. 7, pp. 67-81.

14. **El-Hofy, Hassan.** *Fundamentals of Machining Processes.* Boca Raton, Florida : CRC Press, 2007. 0849372887.

15. **Lopez de Lacalle, L. N., et al.** Recording of real cutting forces along the milling of complex parts. *Mechatronics.* 2006, Vol. 16, 21-32.

16. **Lopez de Lacalle, L. N., et al.** Using high pressure coolant in the drilling and turning of low. *International Journal of Advanced Manufacturing Technology.* 2000, Vol. 16, 85-91.

17. **Tobias, S. A.** *Machine tool vibration.* London, England : Blackie, 1965.

18. **Tlustly, J.** *Dynamics of high speed milling, handbook of high speed.* London, England : Champman and Hall, 1985.

19. **Smith, K. S. and Dvorak, D.** Tool path strategies for high speed milling. *Mechatronics.* 1998, Vol. 8, 291-300.

20. **Chiriacescu, S. T.** *Stability in the Dynamics of Metal Cutting.* New York : Elsevier, 1990.

21. **Fofana, M. S.** Delay dynamical systems and applications to machine-tool chatter. *Chaos, Solitons and Fractals.* 2003, Vol. 17, 731-747.

22. **Fofana, M. S., et al.** Illustrative applications of the theory of delay dynamical systems. *Mathematical and Computer Modeling.* 2003, Vol. 37, 1371-1382.

23. **Fofana, M. S.** Moment Lyapunov exponent of a stochastic delay equation. *International Journal of Mathematics and Mathematical Sciences.* 6, 2002, Vol. 30, 339-351.

24. **Fofana, M. S.** Sufficient conditions for the stability of single and multiple regenerative chatter. *Chaos, Solitons and Fractals.* 2002, Vol. 14, 335-347.

25. **Fofana, M. S.** Aspects of stable and unstable machining by Hopf bifurcation. *Journal of Applied Mathematical Modeling.* 2002, Vol. 26, 953-973.

26. **Fofana, M. S.** Spatial decomposition in a mechanical system with discrete delays. *International Journal of Differential Equations and Applications.* 4, 2000, Vol. 4, 371-395.

27. **Fofana, M. S.** Effects of time delays near center manifold. *International Mathematical Journal.* 3, 2002, Vol. 1, 285-302.

28. **Fofana, M. S. and Lamb, D. L.** On the stability of a nonlinear time delay system. *Automatica Journal.* 3, 1995, Vol. 34, 375-378.

29. **Fofana, M. S., Ee, K. C. and Jawahir, I. S.** Machining stability in turning operation when cutting with a progressively worn tool insert. *Wear.* 2003, Vol. 255, 1395-1403.

30. **Fofana, M. S. and Ryba, P. B.** Parametric stability of nonlinear time delay equations. *International Journal of Nonlinear Mechanics.* 2003, Vol. 39, 79-91.

31. **Hanna, N. H. and Tobias, S. A.** A theory of nonlinear regenerative chatter. *ASME Journal of Engineering for Industry.* 1974, Vol. 96, 247-255.

32. **Shi, H. M. and Tobias, S. A.** Theory of finite amplitude machine instability. *International Journal of Machine Tool Design and Research Conference.* 1, 1984, Vol. 24, 45-69.

33. **Tobias, S. A.** *Machine Tool Vibration.* London : Blackie and Sons Ltd, 1965.

34. *Manufacturing Engineering, Aerospace and Defense Manufacturing.* s.l. : Society of Manufacturing Engineers, 2008.

35. **Heisel, Uwe and Mult, H. C.** Production engineering, research and development. *Annals of the German Academic Society for Production Engineering.* 2, 2006, Vol. 13.

36. **Vieira, J. M., Machado, A. R. and Ezugwu, E. O.** Performance of cutting fluid during face milling of steels. *Journals of Material Process Technology.* 2001, Vol. 116, 244-251.

37. **Xavior, M. A. and Adithan, M.** Determining the influence of cutting fluids on tool wear and surface roughness during turning of AISI 304 austenitic stainless steel. *Journal of Material Process Technology.* 2009, Vol. 209, 900-909.

38. **Belluco, W. and De Chiffre, L.** Performance evaluation of vegetable-based oil in drilling austenitic stainless steel. *Journal of Materials Process Technology.* 2004, Vol. 148, 171-176.

39. **Axinte, D. A. and De Chiffre, L.** Effectiveness and resolution of tests for evaluating the performance of cutting fluids in machining aerospace alloys. *CIRP Annals - Manufacturing Technology.* 2008, Vol. 57, 129-132.

40. **Sales, W. F., et al.** Evaluation of Cutting Fluids Using Scratch Tests and Turning Process. *Journal of the Brazil Society of Mechanical Science and Engineering.* 2007, Vol. 29, 372-378.

41. **Axinte, D., Axinte, M. and Tannock, J. D.** A multicriteria model for cutting fluid evaluation. *Proceedings of the Institution of Mechanical Engineers, Part B: Journal of Engineering Manufacture.* 2003, Vol. 217, 1341-1353.

42. **Ezugwu, E. O., et al.** Machining of nickel-base, Iconel 718, alloy with ceramic tools under finishing conditions with various coolant supply pressures. *Journal of Materials Processing Technology.* 2005, Vols. 162-163, 609-614.

43. **Mazurkiewicz, M., Kubala, Z. and Chow, J.** Metal machining with high-pressure water-jet cooling assistance - a new possibility. *Journal of Engineering for Industry.* 1989, Vol. 111, 7-12.

44. **Sharma, C. S., Rice, W. B. and Salmon, R.** Some effects of injecting cutting fluids directly into the chip-tool interface. *Journal of Engineering for Industry.* 1971, Vol. 93, 441-444.

45. **Taylor, F. W.** On the art of cutting metals. *The Transaction of ASME.* 1906, Vol. 28, 70-350.